# Supporting Information for "Orbital-use fees could more than quadruple the value of the space industry"

Akhil Rao, Matthew G. Burgess, Daniel Kaffine

May 14, 2020

## 1 Extended description of methods and discussion of results

We generate the path of an optimal orbital-use fee (OUF) in three steps. First, we calibrate functions describing the physics and economics of orbit use to match observed data on satellite and debris stock levels and aggregate satellite industry costs and revenues prior to 2015. Then, using the calibrated values, we generate open access and optimal launch paths from 2006 to 2040. Finally, by comparing the open access path of collision risk to the optimal path of collision risk, we calculate the path of the optimal OUF which induces open access satellite owners to internalize the externality they impose on other orbit users. Since the optimal OUF is precisely the marginal external cost of another satellite launched, the final calculation amounts to calculating this marginal external cost.

As we state in the main text, our goal in this article is to provide order-of-magnitude estimates of the optimal OUF and the net present value (NPV) gains from implementing it, and to show the qualitative features of both the OUF path and NPV gains. As we discuss below, our conclusion that a globally-harmonized OUF is necessary to improve the value of the satellite industry is robust to the limitations in our estimation methodology.

We measure the value of the satellite industry as the NPV of cash flows generated by the satellite fleet. NPV accounts for the time value of money — the fact that cash flows received sooner are preferable to cash flows received later — by discounting future cash flows according to the interest that could have been earned on those cash flows had they been received in the present and immediately reinvested in capital markets. In this article, we use the infinite-horizon NPV of the satellite fleet. To calculate this value, we assume that satellite costs and revenues evolve according to the projection in Jonas et al. [12] until 2050, after which they stabilize at 2050 levels and are constant for the infinite future.[1] The resulting NPVs reflect the sum of short- and long-run costs and returns from the satellite fleet. To express these in terms of equivalent constant cash flows received each year, we convert the NPV into an annuitized present value in the main text.[2] For example, given a discount rate of 5%, a net present value of $1 trillion in 2020 is equivalent to an annuitized present value of $47 billion received in perpetuity in each year from 2020 onwards.[3]

We obtain physical functions relating launches, satellites, and debris stocks to collisions, new fragments, and satellite and debris growth from the engineering literature, and economic functions relating the decision to launch to collision risk, costs, and returns from the economics literature. To calibrate the physical functions, we estimate the unknown parameters from satellite stocks, debris stocks, and launches observed over 1957–2014. We constrain the parameters to comply with theoretical restrictions imposed by the engineering model. To calibrate the economic functions, we estimate the unknown parameters from satellite stocks, debris stocks, launches, aggregate satellite in-

[1] The projection in Jonas et al. [12] only goes till 2040 — we extend it to 2050 by calculating the compound annual growth rate of the costs and revenues, and assuming that they continue to grow at those rates from 2040 until 2050.

[2] The annuitized present value (PV) of an NPV level is the constant number of dollars received each year such that the discounted sum of annuitized PVs is equal to the target NPV level. Formally, defining the NPV of a stream of uneven cashflows $x_t$ as $NPV = \sum_{t=1}^{\infty} \beta^{t-1} x_t = \sum_{t=1}^{\infty} \beta^{t-1} A = A(1-\beta)^{-1}$ for some constants $A > 0$ and $\beta \in (0,1)$, the annuitized PV is $A = NPV(1-\beta)$. These conversions facilitate comparisons between uneven streams of cash flows, as they can be expressed in a common unit at a single point in time (NPV terms) or in a common unit at every point in time (annuitized PV terms).

[3] We discuss the interpretation of the discount rate as the opportunity cost of funds invested below.

dustry costs, and aggregate satellite industry returns over 2006–2014.[4] To allow the estimation process to adjust for unobserved launch market frictions, we do not constrain these parameter estimates.

## 1.1 Data

### 1.1.1 Satellite and debris counts, 1957–2014

We use data on satellites in orbit from the Union of Concerned Scientists' (UCS) lists of active satellites to construct the satellite stock and launch rate series [22]. The UCS data provide details on payloads in low-Earth orbit (LEO) and their projected lifetimes. The data are described in Table S1.

| Variable | Sample period | Mean | St. Dev. | Min | Max |
|---|---|---|---|---|---|
| *Active satellite count* | 1957–2014 | 1057.9 | 720.3 | 4 | 2271 |
| *Launch successes* | 1957–2014 | 89.9 | 47.1 | 5 | 334 |
| *Launch failures* | 1957–2014 | 13.8 | 9.8 | 1 | 42 |
| *Payloads decayed* | 1957–2014 | 50.8 | 24.1 | 3 | 90 |
| *Debris-creating anti-satellite missile tests* | 1957–2014 | 0.2 | 0.4 | 0 | 1 |
| *Debris count* | 1957–2014 | 3375.6 | 2681.3 | 0 | 9662 |
| *Expected collision rate (active satellites hit)* | 1957–2014 | 2.6 | 1.8 | 0 | 6 |
| *Historical satellite industry revenues (billion nominal USD)* | 2006–2014 | 101.7 | 20.4 | 70.4 | 126.6 |
| *Historical satellite industry costs (billion nominal USD)* | 2006–2014 | 185.4 | 40.1 | 136.2 | 254.4 |
| *Projected satellite industry revenues (billion nominal USD)* | 2015–2040 | 217.9 | 76.5 | 120.8 | 366.6 |
| *Projected satellite industry costs (billion nominal USD)* | 2015–2040 | 362.2 | 87 | 210.7 | 525.1 |

Table S1: Summary statistics for the data we use to calibrate our physical and economic models and to project open access and optimal launch rates. All values rounded to first non-zero decimal place.

We construct the number of active satellites in each year by calculating the number of objects launched in a particular year, adding the number of satellites previously calculated in orbit, and then subtracting the number of satellites listed as having decayed in that year.[5]

Letting $\ell_t$ be the number of collisions observed in year $t$ and $Z_t$ be the number of payloads listed as decayed in $t$, we construct the launch rate in $t$, $X_t$, from the law of motion for the satellite stock series as

$$\begin{aligned} S_{t+1} &= S_t - Z_t - \ell_t + X_t \\ \implies X_t &= S_{t+1} - S_t + Z_t + \ell_t, \end{aligned} \tag{1}$$

where $S_t$ is the number of active payloads in $t$ and $Z_t$ is the number of payloads listed as decayed in $t$.

The debris and collision risk series' we use were provided by the European Space Agency. We use debris data from the DISCOS database [8] and collision probability data used in Letizia et al. [18] (the variable $p_c$ in that paper).

[4] While we have physical data series extending till 2017, and economic data series covering 2005–2015, we omit observations after 2014 in all calibration data and the 2005 observations in the economic data series. Equations 7 and 14 are the bottlenecks: the former requires omission of the first year's data to construct the cost growth variable, while the latter cannot be used to construct the necessary implied cost growth for the final year. As a result, our economic data calibration only uses data covering 2006–2014. Since our economic model implies that the number of objects in orbit and the collision risk convey economic information about returns and costs, we omit physical variables after 2014 from our physical model calibration to avoid unintended data snooping.

[5] This procedure is likely to produce an upward-biased estimate of the returns-generating satellite stock in any given year, since satellites which are no longer operational will not be removed from the estimated stock until they have deorbited. Thus, the satellite stock in this procedure includes some objects which are, economically speaking, "socially-useless debris". We use this procedure despite the attribution issue for two reasons. First, we do not have data on when specific satellites were declared nonoperational by their owners. Such a determination can be particularly tricky when a mission has ended, but the satellite still has fuel and could be repurposed for another mission. Second, to the extent that our estimates of the satellite stock are biased upward (toward positive infinity), our physical and economic parameters estimates will be biased downwards. The downward bias in economic parameters will deflate both the open access and socially optimal launch rates, while the downward bias in physical parameters will inflate both the open access and socially optimal launch rates, with the net effect being difficult to determine. However, the downward bias in our estimated collision risk coefficients and the upward bias in our estimated satellite stock will bias our estimated OUF downward, so that it is a lower bound.

We use only objects with a semi-major axis of 2000km or less in all our data series. We prefer to use the DISCOS fragment data rather than the Space-Track fragment data [6] as DISCOS attributes fragments to the time they were created or detected, whereas the Space-Track data attributes fragments to the time their parent body was launched. The DISCOS attribution method is closer to how economic agents in our model receive information and make decisions. Given the difficulties in determining operational status, the collision probability estimates account for the probability of collisions with all intact bodies. This produces an upward-biased estimate of the probability of collisions with only operational satellites. This upward bias likely deflates the number of open access and optimal launches we project. However, since the open access and optimal launch rates are chosen to equate collision risk with measures of economic returns (described in equations 6 and 9), the resulting estimated OUF paths will not be biased upward by the same degree as the collision probability estimates.

The historical time-series of destructive hit-to-kill anti-satellite missile tests we use was compiled by Brian Weeden of the Secure World Foundation, and provided to us by Laura Grego [3]. It is the most comprehensive dataset we are aware of regarding anti-satellite missile and ballistic missile defense tests. Since our ASAT parameter represents the number of fragments created by a missile destroying a satellite, we ignore tests recorded as creating no debris (e.g. tests in which the missile only passed through a chosen point in space and then fell into the ocean) and only use those which were recorded as creating debris. The original data only records fragments cataloged by the U.S military, generally fragments 10cm in size or larger. As a result, there could be additional tests which created debris too small to track which we do not account for. Improvements in radar systems used for space situational awareness after 2003 also result in higher numbers of fragments detected after 2003 (implying fragment counts before 2003 were likely understated in the data). These factors, combined with the likelihood of too-small-to-track fragments from known destructive tests, likely bias our estimated ASAT parameter toward zero.

### 1.1.2 Aggregate satellite industry returns and costs, 2006–2040

We use data on historical satellite industry revenues from Wienzierl [24], and UCS data on satellites in LEO (semi-major axis less than 2000km) [22]. The economic data provide a breakdown of revenues across satellite manufacture, launch, insurance, and products and services. The satellite industry revenues data cover 2006-2015, while the active satellites data cover 1957-2014. To generate launch rate and OUF projections out to 2040, we use revenue and cost projections from Jonas et al. [12]. These projections are shown in Figure 1a of the main text. The historical and projected data we use are described in Table S1.

We calculate the per-period returns on owning a satellite ($\pi_t$) as the revenues generated from commercial space products and services, and the per-period costs of building, launching, and operating a satellite ($F_t$) as the sum of revenues from commercial infrastructure and support industries, ground stations and equipment, commercial satellite manufacturing, and commercial satellite launching. The ratio $\pi_t/F_t$ then gives a time series of the rate of return on a single satellite, as the number of satellites cancels out of the numerator and denominator.[6] Since the numbers provided in Wienzierl [24] are for the satellite industry as a whole, the ratio still needs to be adjusted to represent satellites in LEO. We do not explicitly conduct this adjustment, but let the adjustment be calculated during the estimation of equation 7.[7]

Note that the data we use for $\pi_t$ and $F_t$ are industry-level aggregates, rather than satellite-level figures. To convert the data from industry-level figures to per-satellite figures, we must apply a scaling factor which "disaggregates" the data. This unknown factor is common to both cost and revenue aggregates, and so cancels out of $\pi_t/F_t$ such that the ratio correctly represents the rate of return per satellite. Since we use $\pi_t/F_t$ to compute the open access and optimal policy and value functions, the unknown scaling factor does not affect our solutions (launch rates). However, it does affect our calculated time paths of NPV under business-as-usual (BAU, i.e. open access) and optimal management as well as the OUF, since those values do not involve ratios which would cancel out the unknown scaling factor. Since the unknown scaling factor is on the order of the reciprocal of the number of satellites in orbit (or projected to be in

[6] This is true whether the satellites were launched individually on separate rockets or in groups on the same rockets.

[7] Another way to perform this adjustment is by calculating the yearly share of satellites in LEO and multiplying the ratio $\pi_t/F_t$ by the share in LEO. This approach is difficult to generalize to future years since it requires projections of satellites in other orbits. It is also not clear that the returns of satellites in LEO are truly proportional to the LEO share of the total number of active satellites in all orbits; it seems more likely that LEO satellites earn less revenue per satellite than geostationary satellites.

orbit) in each period, we proxy for it in our projected time paths by dividing by the BAU satellite stock path. This choice of proxy does not affect our qualitative results or the order of magnitude of the OUF or NPV under BAU and optimal management—using alternate proxies such as the optimal management path of satellites or the observed number of satellites in 2015 produces similar results, although our proxy results in more conservative projections than those alternative choices.

## 1.2 Models

### 1.2.1 Orbital mechanics with limited lifespans, missile tests, and certainty

Our physical model uses physical accounting relationships in the aggregate stocks of satellites and debris for the laws of motion, and draws on [17] for the functional forms of the new fragment creation and collision probability functions $G(S,D)$ and $L(S,D)$. The time scale is set as one calendar year to match our data. $S_t$ denotes the number of active satellites in an orbital shell in period $t$, $D_t$ the number of debris objects in the shell in $t$, $X_t$ the number of satellites launched in $t$, $L(S_t,D_t)$ the probability that an active satellite in the shell will be destroyed in a collision in $t$, $\mu$ is the fraction of satellites which do not deorbit in $t$, and $m$ is the average amount of debris generated by launching satellites (such as rocket bodies). $\delta$ is the average proportion of debris objects which deorbit in $t$, and $G(S_t,D_t)$ is the number of new debris fragments generated due to all collisions between satellites and debris.[8] $A_t$ is the number of anti-satellite missile tests conducted in $t$, and $\gamma$ is the average number of fragments created by one test. We assume that satellites which deorbit do so without creating any additional debris.

In the real world, satellite operators typically take evasive action to avoid debris. The collision probability function $L$ should therefore be interpreted as the probability of a collision which is not avoided, either because it is unavoidable, the avoidance maneuver did not succeed, or because it would be too costly to do so. A more detailed model would separate the probability of collisions into the probability of a physical collision event and the probability of an unsuccessful avoidance maneuver; we lack sufficient data to make this distinction. Modeling the failure rate of avoidance maneuvers is an important area for future research.

The number of active satellites in orbit is modeled as the number of launches in the previous period plus the number of satellites which survived the previous period (also shown in equation 1). The amount of debris in orbit is the amount from the previous period which did not decay, plus the number of new fragments created in collisions, plus the amount of debris in the shell created by new launches.[9] Formally,

$$S_{t+1} = S_t(1 - L(S_t,D_t))\mu + X_t \tag{2}$$

$$D_{t+1} = D_t(1-\delta) + G(S_t,D_t) + \gamma A_t + mX_t. \tag{3}$$

For simplicity, we assume all non-operational satellites are immediately deorbited, making our OUF estimates conservative. [17] use an analogy to kinetic gas theory to parameterize the probability of a collision as a negative exponential function, with the density of colliding objects one of the arguments of the exponential function. We therefore parameterize $L(S_t,D_t)$ as

$$L(S_t,D_t) = 1 - \exp(-\alpha_{SS}S_t - \alpha_{SD}D_t), \tag{4}$$

where $\alpha_{SS}$ and $\alpha_{SD}$ include the difference in velocities between the objects colliding, the total cross-sectional area of the collision, and scaling parameters which relate the number of objects to their density in the volume. We use these probability functional forms to parameterize $G(S_t,D_t)$ as

$$G(S_t,D_t) = \beta_{SS}(1-\exp(-\alpha_{SS}S_t))S_t + \beta_{SD}(1-\exp(-\alpha_{SD}D_t))S_t, \tag{5}$$

[8] For most of our sample, the number of observed collisions is zero. We use the probability of collisions in our models rather than the observed number for two reasons. First, it proxies for unobserved collisions, including non-catastrophic ones. Second, a model with stochastic collisions complicates the process of solving for the optimal time path by adding another state variable to the dynamic programming algorithm. As the number of objects in a single period increases, the fraction of satellites destroyed in collisions in that period converges to the probability of destruction, so this assumption provides a "mean field"-type approximation.

[9] Empirically, we only consider the population of trackable fragments, i.e. those with size greater than 5-10cm in LEO.

where the $\beta_{jk}$ parameters are interpreted as "effective" numbers of fragments from collisions between objects of type $j$ and $k$.[10] We refer to the $\alpha_{jk}$ and $\beta_{jk}$ as "structural physics parameters", as they represent physical entities which are exogenous to our model.

We ignore the possibility of collisions between debris objects for two reasons. First, the data we have do not allow us to identify the effective number of fragments from such collisions, or the probability of such collisions, using our calibration approach. Second, our focus here is not on the probability of Kessler Syndrome, but on launch patterns and their response to the extant stock of orbiting satellites and debris. Our estimates of the optimal OUF path and the benefits of implementing it are likely understated due to this omission. Incorporating the possibility of Kessler Syndrome is an important piece of optimal orbit use analysis and policy design, and will likely require higher-fidelity physical modeling than the "aggregate calibration" approach we take here. This is an important area for future research.

Equations 3, 4, and 5 can be viewed as reduced-form statistical models which recreate the results of higher-fidelity physics models of debris growth and the collision probability. While higher-fidelity physics models may use similar functional forms, the key difference between our approach and the approach in such models is how we calibrate the models: rather than derive the appropriate parameter values from physical first principles given the data, we estimate the values of those parameters which maximize the fit between the data and model-predicted collision probabilities, satellite evolution, and debris stocks. Though our approach is computationally convenient, it likely sacrifices some predictive power.

While we model a collision probability, we do not formally include uncertainty (e.g. as a probability measure over collisions to be integrated) in the decision-making processes of satellite launchers/operators. Formal uncertainty of this type could be important when modeling untracked debris. However, our data do not include estimates of untracked debris. Our lack of formal uncertainty could therefore be interpreted as assuming all data are tracked. We also do not observe the history of near-hits, making it challenging to calibrate the stochastic process of collision events directly. Finally, the linearity of per-period profit functions in our model suggests behavioral effects like risk aversion will not matter to launch rates.

### 1.2.2 Open access orbit use with time-varying aggregate returns and costs

The economic model of open access here is based on the model of open access in [21] to determine the satellite launch rate under open access, $X_t$, as a function of the collision probability, $L(S_{t+1}, D_{t+1})$, and the excess return on a satellite, $r_s - r$.[11] We derive the following equilibrium conditions, equations 6 and 7, in section 1.7. In the simplest case, where all of the economic parameters are constant over time and satellites are infinitely lived, the open access launch rate equates the collision probability with the excess return:

$$L(S_{t+1}, D_{t+1}) = \underbrace{r_s - r}_{\substack{\text{excess return} \\ \text{on a satellite}}} , \tag{6}$$

where $r_s$ is the per-period rate of return on a single satellite ($\pi/F$), where $\pi$ is the per-period return generated by a satellite and $F$ is the cost of launching a satellite, inclusive of non-launch expenditures such as satellite manufacturing and ground stations) and $r$ is the risk-free interest rate.[12]

Equation 6 can therefore also be used to calculate the implied internal rate of return (IRR) for satellite investments from observed data on collision risk and satellite returns. $r$ is not observed in our data. When costs and returns are

[10] "Effective" numbers of fragments measure the number of new fragments weighted by the time they spend inside the volume of interest. This approach is used in the debris modeling literature, for example [2].

[11] While we consider LEO as a whole, this approach could be generalized to individual spherical shells within LEO. Such generalization could incorporate the substantial heterogeneity in orbital-use values. For example, some orbits are more valuable because they offer ideal conditions for Earth observation, and will likely need a different fee schedule than orbits which do not offer such conditions.

[12] More precisely, $r$ is the opportunity cost of funds invested in launching a satellite, and may diverge from the risk-free rate if the satellite launcher's most-preferred alternate investment is not a risk-free security. This rate is sometimes referred to as the internal rate of return.

time-varying, equation 6 becomes

$$L(S_{t+1},D_{t+1}) = 1 + r_{s,t+1} - (1+r)\frac{F_t}{F_{t+1}} \tag{7}$$
$$\implies L(S_{t+1},D_{t+1}) = \underbrace{\left(r_{s,t+1} - r\frac{F_t}{F_{t+1}}\right)}_{\substack{\text{excess return}\\ \text{on a satellite}}} + \underbrace{\left(1 - \frac{F_t}{F_{t+1}}\right)}_{\substack{\text{capital gains}\\ \text{from open access}\\ \text{and satellite launch}\\ \text{cost variation}}}$$

where $r_{s,t+1} = \pi_{t+1}/F_{t+1}$. With time-varying economic parameters, two sources of returns drive the collision risk. One is the excess return realized in $t+1$ from launching a satellite in $t$. The other is the capital gain (or loss) due to open access and the change in satellite costs. Since open access drives the value of a satellite down to the total cost of launching and operating it, $F_t$ becomes the cost of receiving $F_{t+1}$ in present value the following period, and the returns are given as percentages of $F_{t+1}$. Since the discount rate is unobserved, we fix it to be constant over time to facilitate estimation.[13] While we abstract from the fact that satellite lifetimes are finite in equation 7, we account for it in our calibration. We discuss this issue further when describing our calibration methodology in section 1.3.2, including why it is unlikely to affect our estimates of the optimal OUF and the benefits of implementing it.

### 1.2.3 Optimal orbit use with time-varying aggregate returns and costs

Determining the launch plan to ensure optimal orbit use is more complicated. Economists commonly refer to this type of problem as "the (fleet) planner's problem", imagining a planner tasked with maximizing fleet-wide NPV. The fleet planner launches satellites to maximize the value of the entire fleet into the (discounted) infinite future, subject to the laws of motion of satellite and debris stocks. Formally, letting $\beta = (1+r)^{-1}$ be the discount factor, the planner solves

$$\begin{aligned} W_t(S_t,D_t) &= \max_{X_t \geq 0}\{\pi_t S_t - F_t X_t + \beta W_{t+1}(S_{t+1},D_{t+1})\} \\ S_{t+1} &= S_t(1 - L(S_t,D_t))\mu + X_t \\ D_{t+1} &= D_t(1-\delta) + G(S_t,D_t) + \gamma A_t + mX_t. \end{aligned} \tag{8}$$

The economic parameters $\pi$ and $F$ are allowed to be time-varying in our solution approach, though all other physical and economic parameters are constant over time.[14]

Solving the planner's problem by taking the first-order condition and applying the envelope condition to recover the unknown functional derivatives, we obtain an expression for the collision risk in period $t+1$ which characterizes the optimal launch rate in period $t$:

$$L(S_{t+1},D_{t+1}) = 1 + r_{s,t+1} - (1+r)\frac{F_t}{F_{t+1}} - \xi(S_{t+1},D_{t+1}), \tag{9}$$

where

$$\begin{aligned} \xi(S_{t+1},D_{t+1}) = S_{t+1}L_S(S_{t+1},D_{t+1})\mu F_{t+1} + \frac{\pi_t - rF_t - L(S_t,D_t)\mu F_t - S_t L_S(S_t,D_t)\mu F_t}{\beta(1-\delta+G_D(S_{t+1},D_{t+1}) + mL_D(S_{t+1},D_{t+1})\mu S_{t+1})} \\ - \frac{\beta G_S(S_{t+1},D_{t+1}) + m(1 - L(S_{t+1},D_{t+1}) - S_{t+1}L_S(S_{t+1},D_{t+1}))\mu}{\beta(1-\delta+G_D(S_{t+1},D_{t+1}) + mL_D(S_{t+1},D_{t+1})\mu S_{t+1})} L_D(S_{t+1},D_{t+1})\mu S_{t+1}F_{t+1} \end{aligned} \tag{10}$$

is defined as the marginal external cost of another satellite. These equations are derived in Section 1.8.

[13] This equation was derived in the Appendix of [21]. In that setting the discount rate was not constant over time.

[14] While the convention in infinite-horizon dynamic programming is to drop time subscripts and use primes on a variable's right to indicate future values, we use time subscripts here to avoid cluttering the state vector with changing parameters and to clearly show which values are changing over time.

## 1.3 Calibration and simulation

### 1.3.1 Physical parameters: deorbit, decay, collisions, and fragments

We calibrate the rate at which satellites deorbit, $\mu$, by estimating the following analog to equation 1 by ordinary least squares (OLS):

$$S_{t+1} = S_t(1 - L(S_t, D_t))\hat{\mu} + X_t + \varepsilon_{St}. \tag{11}$$

We use hats over variables to indicate a parameter being estimated, e.g. $\mu$ is the true (unknown) value while $\hat{\mu}$ is the estimate of $\mu$.$\varepsilon_{St}$ is the error term.

Equation 11 yields an estimated average lifespan of about 30 years, i.e. $\hat{\mu} = 0.967$. This is consistent with an average mission length of 5 years, followed by compliance with the 25-year deorbit guideline issued by the IADC [11]. Using this rate in our forward simulations is conservative in the sense that the estimated OUF becomes a lower bound relative to a model with imperfect compliance. Bradley and Wein [2] show full compliance to be optimal.

We calibrate equations 3 and 4 by estimating the following equations:

$$L(S_t, D_t) = 1 - \exp(-\hat{\alpha}_{SS}S_t - \hat{\alpha}_{SD}D_t) + \varepsilon_{Lt} \tag{12}$$

$$D_{t+1} = (1 - \hat{\delta})D_t + \hat{\beta}_{SS}(1 - \exp(-\hat{\alpha}_{SS}S_t))S_t + \hat{\beta}_{SD}(1 - \exp(-\hat{\alpha}_{SD}D_t))S_t + \hat{\gamma}A_t + \hat{m}X_t + \varepsilon_{Dt}. \tag{13}$$

Theory predicts $\alpha_{jk}$, $\beta_{jk}$, and $m$ are nonnegative, and $\delta$ is in $(0,1)$. We constrain the parameter estimates to comply with the theoretical restrictions.

We estimate equations 12 and 13 in two stages. First, we estimate equation 12 by constrained nonlinear least squares (NLS). Then, using the estimated values of $\hat{\alpha}_{SS}$ and $\hat{\alpha}_{SD}$ to generate $(1-\exp(-\hat{\alpha}_{SS}S_t))S_t$ and $(1-\exp(-\hat{\alpha}_{SD}D_t))S_t$, we estimate equation 13 by constrained ridge regression, estimating $(1-\delta)$ directly.[15] We estimate both equations on the sample from 1957-2014. The fitted values for all three equations are shown against the actual values in Figure S1.

Tables S2 and S3 show the calibrated parameters for equations 12 and 13. Since our goal is predicting the time series rather than inference on the physical coefficients, we focus on prediction uncertainty estimates for equations 12 and 13 in Figure S3 rather than coefficient standard errors.

| **Collision probability parameters** | $\alpha_{SS}$ | $\alpha_{SD}$ |
|---|---|---|
| *Parameter values* | 1.29e-06 | 2.56e-08 |
| *Standard errors:* | 1.61e-07 | 4.90e-08 |

Table S2: Parameter values and standard errors from estimating equation 12. Standard errors are computed from residual-bootstrapped parameter sets. The residual bootstrap procedure is described in section 1.4.

| **Debris law of motion parameters** | $\delta$ | $m$ | $\gamma$ | $\beta_{SS}$ | $\beta_{SD}$ |
|---|---|---|---|---|---|
| *Parameter values* | 0.50 | 4.38 | 462.47 | 292.68 | 5159.58 |
| *Standard errors* | 0.003 | 0.04 | 0.37 | 39.57 | 5807.69 |

Table S3: Parameter values and standard errors from estimating equation 13. All values are rounded to two decimal places. The penalty parameter $\lambda$ was selected through cross-validation. Standard errors are computed from residual-bootstrapped parameter sets. The residual bootstrap procedure is described in section 1.4.

Values estimated for equation 13 are lower bounds due to ridge estimation bias. For example, the value of $m$ suggests that every satellite launched creates at least 4.38 pieces of debris on average, while the value of $\gamma$ suggests that when anti-satellite missile tests create debris they create at least 462.47 pieces of debris on average.

[15] We use ridge regression for the debris equation to improve the model's out-of-sample predictive performance, despite bias in the estimated parameters and potentially poorer in-sample fit [10, 26]. Ridge estimates are biased toward zero relative to OLS estimates. For a given penalty parameter $\lambda \geq 0$, the relationship between a ridge coefficient estimate $\hat{\beta}^{\text{ridge}}$ and the corresponding OLS estimate $\hat{\beta}^{\text{OLS}}$ is $\hat{\beta}^{\text{ridge}} = \hat{\beta}^{\text{OLS}}/(1+\lambda)$.

### 1.3.2 Economic parameters: returns, costs, and discounting

While we observe the total revenues for various sectors of the satellite industry, we do not have sufficient data to (a) disentangle the revenues arising due to LEO operators from those of other operators, or (b) accurately model the market structures of the various sectors of the satellite industry. We also do not observe the discount rate used by LEO satellite operators. Consequently, the data we use for $F_t$ and $\pi_t$ must be adjusted in an unknown fashion to account for these issues before they can be used to project open-access launch rates to LEO.

Fortunately, equation 7 offers an equilibrium relationship which can provide us with reduced-form "adjustment coefficients" that reflect a combination of the unobservable factors we mention above. We therefore calibrate equation 7 by estimating

$$L(S_t, D_t) = a_{L1} + a_{L2} r_{st} + a_{L3} \frac{F_{t-1}}{F_t} + \varepsilon_{rt}, \tag{14}$$

using OLS on the sample of returns data from 2005-2015, omitting the first observation (for 2005) to construct $F_{t-1}/F_t$. $\varepsilon_{rt}$ is a mean-zero error term, $a_{L2}$ is a scale parameter, and $a_{L3}$ measures the gross IRR, $1+r$. We do not explicitly incorporate satellite lifetimes net of exogenous failure (the parameter $\mu$) as the coefficient is not separately identifiable — it enters each term in equation 14 as a scalar multiplying the parameters $(a_{L1}, a_{L2}, a_{L3})$, and does not affect the model's predictions. Table S4 shows the calibrated parameters.

| **Economic calibration parameters** | $a_{L1}$ | $a_{L2}$ | $a_{L3}$ |
|---|---|---|---|
| *Parameter values* | 0.004 | 0.009 | -0.0004 |
| *Standard errors* | 0.002 | 0.002 | 0.001 |

Table S4: Parameter values from estimating equation 14. All values are rounded to the first non-zero digit.

If our data perfectly measured the costs and returns of satellite ownership, and our theoretical model held exactly, we would expect $a_{L1} = 1$, $a_{L2} = 1$, and $a_{L3} < -1$. Our estimates therefore suggest that our returns and cost series are measured with error or that our theoretical model is missing some important factors. Some potential factors include binding launch constraints, cost efficiencies in satellite production, market power in the launch industry, or vertical integration between launch providers and satellite operators. Further empirical research on the structure of the satellite and launch industries is needed to disentangle these potential explanations.

To account for these missing factors in the historical period, we calibrate our satellite launch cost data to be consistent with the simple open access model by using the estimated parameter values from the economic calibration. Table S5 compares the calibrated data to the original series. The calibrated cost data are of the same magnitude as the uncalibrated data, but typically smaller. This suggests that the unmodeled factors include cost efficiencies in satellite production, launch, and management, or constraints on launch services available each period, which are consistent with the analytical features we abstract from in our theoretical model.

Regardless of the specific factors missing from the theoretical model, we use equation 14 to recursively calibrate the sequence of launch costs implied by the combination of open access, observed launch rates, and observed satellite returns as

$$\begin{aligned} L(S_t, D_t) &= a_{L1} + a_{L2} r_{st} + a_{L3} \frac{F_{t-1}}{F_t} + \varepsilon_{rt} \\ \implies L_t &= a_{L1} + a_{L2} \frac{\pi_t}{F_t} + a_{L3} \frac{F_{t-1}}{F_t} + \varepsilon_{rt} \\ \implies \hat{F}_t &= \frac{a_{L2}\pi_t + a_{L3} F_{t-1}}{L_t - a_{L1}}. \end{aligned} \tag{15}$$

This "calibrated cost" accounts for these missing factors in the historical period. When it exceeds the observed costs, the missing factors tend to reflect unobserved costs to launching satellites, such as limited launch availability. When it is below the observed costs, the missing factors tend to reflect unobserved returns to launching satellites, such as returns to scale.

Table S5 shows the observed satellite returns ($\pi_t$), observed launch costs ($F_t$), and implied launch costs ($\hat{F}_t$). The calibrated costs can be interpreted as the costs such that observed launch patterns result from open access under a non-binding launch constraint and with no other unmeasured factors impacting launch costs. Using the calibrated costs instead of the observed costs in the historical sample ensures that our parameter estimates are consistent with our model of open access.[16]

| Year | Observed aggregate cost | Calibrated aggregate cost |
|---|---|---|
| *2006* | 161.02 | 194.26 |
| *2007* | 185.5 | 178.88 |
| *2008* | 170 | 154.86 |
| *2009* | 137.81 | 131.47 |
| *2010* | 136.16 | 140.48 |
| *2011* | 166.99 | 149.09 |
| *2012* | 186.88 | 165.69 |
| *2013* | 215.9 | 170.79 |
| *2014* | 254.39 | 170.68 |

Table S5: Launch costs (inclusive of satellite construction, integration, and maintenance) implied by open access and observed revenues and costs. Since aggregate launch costs do not reflect the various unmodeled frictions (changing shadow price of the launch constraint, economies of scale in satellite launching, and the share of satellites which are in LEO), we calibrate the economic costs to the collision probability and use the calibration to back out implied costs that reflect these frictions. All values are given in billions of nominal US dollars per year. 2015 is omitted due to the recursive nature of equation 15.

We must still set a value for $r$ explicitly in order to solve the planner's problem. We set the discount rate to be 5% ($r = 0.05$, implying a discount factor of $\beta = (1+r)^{-1} \approx 0.95$). This is intended to be a conservative estimate of a market rate of return, since our planner is effectively an industry planner maximizing the value of the orbit to the satellite and launch industry.

### 1.3.3 Algorithms for open access and optimal policy functions

We generate two sequences of policy functions: one function for each period under consideration, and one sequence for each management regime type. We compute each sequence through backwards induction: beginning at the final period in our projection horizon, and iteratively working backwards to the initial period. This procedure implies "perfect foresight" planning under each management regime, i.e. that all agents under any management regime are able to perfectly forecast the sequence of returns, costs, interest rates, launch rates, and other model objects. The perfect foresight assumption is clearly unrealistic, but our purpose is not to show how uncertainty in economic parameters propagates over time. Rather, our purpose is to show how an optimal OUF would vary over time and the time paths of orbital aggregate stocks under different management regimes. Such assumptions are used in integrated assessment models of climate change with similar rationales, e.g. the models studied in Kelly and Kolstad [13], Nordhaus [20], Wilkerson et al. [25]. Our work here is conceptually similar to integrated assessment modeling.

To compute the open access time path, we first generate a grid of satellite and debris levels, $(grid_S, grid_D)$. We generate this grid as an expanded Chebyshev grid to reduce numerical errors from interpolation, provide higher fidelity near boundaries, and economize on overall computation time [4]. In contrast to a standard Chebyshev grid, an expanded Chebyshev grid allows for computation (rather than extrapolation) at the boundary points. The formula for the $k^{th}$ expanded Chebyshev node on an interval $[a,b]$ with $n$ points is

$$x_k = \frac{1}{2}(a+b) + \frac{1}{2}(b-a)\sec\left(\frac{\pi}{2n}\right)\cos\left(\frac{k}{n} - \frac{1}{2n}\right)$$

We set different values of $b$ for $S$ and $D$, creating a rectangular grid. The main issue in setting $b$ is ensuring that the time paths we solve for (described in section 1.3.4) do not run into or beyond the boundary. To avoid this issue while minimizing the number of points in regions the time paths never reach, we set different $b$ bounds for open access and

[16] Estimating the economic parameters using an open access model with a binding launch constraint is challenging as equation 6 becomes an inequality, giving sets of open access-consistent parameters rather than a unique combination.

the optimal plan, with the open access grid being strictly larger in both dimensions than the optimal plan grid.

In general, computing decentralized solutions under open access is simpler than computing the planner's solutions. This is because open access simplifies the continuation value to the cost of launching a satellite. We use `R` for all simulations, parallelizing where possible. To facilitate convergence of policy and value functions, we normalize the returns and costs parameters so that $\pi_1 = 1$ during computation, and rescale the parameters after the time paths have been generated.

We compute optimal value functions by value function iteration on the grid.[17] We initialize the algorithm with a guess of the value and policy functions. Then, at each point on the grid, we solve the first-order condition for the planner's problem (equation 9). Since there may be multiple solutions, only one of which leads to a global maximum, we then evaluate the value function at each solution (including zero) and select the launch rate attached to the largest level of the value function. Algorithm 1 describes how we compute the optimal policy and value functions for a given grid and given value function guess $guess(S,D)$, while algorithm 2 describes how we compute the open access policy and value functions.

We construct our initial guess of the planner's value function as the terminal value of the fleet. In the penultimate period, we assume it is not optimal to launch any satellites ($X^*_{T-1} = 0$), making the final fleet size

$$S_T = S_{T-1}(1 - L(S_T, D_T)).$$

In the final period ($T$), the payoff of the fleet is $\pi_T S_T$. Our assumption that it is not optimal to launch any satellites in the penultimate period implies the one-period returns of a satellite do not cover the cost of building and launching ($\beta \pi_T < F_{T-1}$), which we verify to hold in every period of our data. We use the implied series of $F_t$ given the observed $\pi_t$ and launch rate series in solving for open access and optimal policies.

**Algorithm 1:** Value function iteration

Set

$$W_0(S,D) = guess(S,D),$$
$$X_0 \equiv 0$$

for all $(S,D) \in (grid_S, grid_D)$

Set $i = 1$ and $\delta = 100$ *(some large initial value).*

**while** $\delta > \varepsilon$ **do**

  At each grid point in $(grid_S, grid_D)$, use a numerical rootfinder to obtain

$$X_i : W_D(S,D) + SL_D(S,D)\hat{F} - \beta[1 - \delta + G_D(S,D) + mSL_D(S,D)]W_D(S',D') = 0,$$

  where $W_D(S,D)$ is given by equation 51.

  Evaluate $W_i(S,D) = \pi S - \hat{F}X_i + \beta W_{i-1}(S',D')$ at $X_i \cup \{0\}$, and select whichever value of $X_i \cup \{0\}$ maximizes $W_i(S,D)$. $W_{i-1}(S',D')$ is computed by linear interpolation.

  $\delta \leftarrow ||W_i(S,D) - W_{i-1}(S,D)||_\infty$.

  i $\leftarrow$ i+1

**end**

### 1.3.4 Projected time paths

We use algorithms 1 and 2 to compute policy and value functions in each period, and run them sequentially from the final period to the first period to generate a series of policy and value functions for each period's set of economic

[17] We prefer value function iteration over straightforward nonlinear programming here for two reasons. First, value function iteration allows us to exploit the parallel structure of the dynamic programming problem to reduce computation time. Second, value function iteration allows us to concentrate computational effort in periods and regions of the state space where it is most useful, avoiding wasted computation time.

**Algorithm 2:** Open access launch plan computation

Use a numerical rootfinder to find the $X^o_{t-1}$ which solves

$$L(S_t, D_t) = a_{L1} + a_{L2}\hat{r}_{st} + a_{L3}\frac{\hat{F}_{t-1}}{\hat{F}_t},$$

using the estimated laws of motion for $S_t$ and $D_t$ as functions of $X_{t-1}$, and the estimated function for $L(S_t, D_t)$.

Approximate $W^\infty_i(S,D) = \sum_{t=1}^{\infty} \beta^{t-1}(\pi S_t - \hat{F} X^o_t)$ as $W^T_i(S,D) = \sum_{t=1}^{T-1} \beta^{t-1}(\pi S_t - \hat{F} X^*_t)$ by backwards induction, using the estimated laws of motion for $S_{t+1}$ and $D_{t+1}$ and the estimated function for $L(S_t, D_t)$. We use $T = 500$.

parameters. Algorithm 3 describes this process.

**Algorithm 3:** Generating a perfect-foresight sequence of policy functions

Set economic parameters to final period values.
Run algorithm 1 (for an optimal path) or 2 (for an open access path) to obtain $W_T(S_T, D_T)$.
**for** *t in T-1:1* **do**
    Set $i = 1$ and $\delta = 100$ *(some large initial value).* Set $X_{0t} = X_T$. **while** $\delta > \varepsilon$ **do**
        Using the value function from the previous time step as $W_{t+1}(S_{t+1}, D_{t+1})$, calculate

$$X^*_{it} : W_{Dt}(S_t, D_t) + S_t L_D(S_t, D_t)\hat{F}_t -$$
$$\beta[1 - \delta + G_D(S_t, D_t) + mS_t L_D(S_t, D_t)] W_{Dt}(S_{t+1}, D_{t+1}) = 0,$$
(for an optimal path, where $W_{Dt}(S,D)$ is given by equation 51),

        or

$$X^o_{it} : L(S_{t+1}, D_{t+1}) = a_{\ell 1} + a_{\ell 2}\hat{r}_{st} + a_{\ell 3}\frac{\hat{F}_{t-1}}{\hat{F}_t} \quad \text{(for an open access path)},$$

        using the estimated laws of motion for $S_{t+1}$ and $D_{t+1}$, the estimated function for $L(S_t, D_t)$, linearly interpolating to compute $W_{t+1}(S_{t+1}, D_{t+1})$.
        $\delta \leftarrow ||X_{it} - X_{i-1t}||_\infty$
    **end**
    If calculating an optimal path, set $W_t(S_t, D_t) = \pi_t S - \hat{F}_t X^* + W_t(S^*_{t+1}, D^*_{t+1})$. If calculating an open access path, set $W_t(S_t, D_t) = \pi_t S - \hat{F}_t X^o + W_t(S^o_{t+1}, D^o_{t+1})$.
**end**

It is important to note that when obtaining the sequence of policy functions we do not do backwards induction within each economic time period prior to the final period. Instead, we hold the continuation value ($W(S_{t+1}, D_{t+1})$) fixed and iterate on the policy functions, using previous iterations' policies as starting points. This ensures that the continuation value incorporates each period's returns and costs only once until the final period, while allowing for any numerical errors in initial policy solves to be corrected. This type of "policy iteration" typically takes 1-2 iterations to converge to within $1e$-3. Backwards induction on the value function in the final period treats that period's costs and returns as steady state values. This is why we change the notation for the fleet value function for algorithm 3, indexing by time to indicate that the launch cost and satellite per-period return are changing in each period.

Once we have a sequence of policy functions for each period's economic parameters, we generate time paths by picking a starting condition $(S_0, D_0)$, computing the launch rate $X_0$ by thin-plate smoothing spline interpolation of the policy function, using the launch rate to compute the next-period state variables, and repeating the process until the terminal period [7].[18] Figure 3 of the main text shows the simulated open access and optimal paths of launches,

[18] Thin-plate smoothing splines are a generalization of cubic splines for multiple dimensions. They are used as multidimensional interpolants,

satellites, debris, and collision risk over the in-sample period, 2005-2015, as well as projections from 2016-2040.

### 1.3.5 Projecting launch availability constraints

The maximum number of satellites which can be launched in a year are limited by a variety of factors, including weather, availability of rockets, and availability of launch sites. To prevent the model from violating the limited availability of launches, we estimate the launch constraint from the observed historical data and then project it forward. In each historical period, we calculate the maximum number of satellites which can be launched as the cumulative maximum of launch attempts (successes+failures). From the historical calculation, we project the launch constraint forward with a linear time trend and an intercept. Table S6 shows the estimated coefficients, and Figure S2 shows the projected launch constraint time path.

| **Launch constraint model parameters** | **Intercept** | **Time trend** |
|---|---|---|
| *Parameter values* | 30.13 | 12.5 |
| *Standard errors* | 16.43 | 2.65 |

Table S6: Parameter values from linear model of launch constraint. All values are rounded to two decimal places. We estimate these coefficients using OLS on the historical launch constraint.

In the historical period, we use the adjusted launch costs (described in section 1.3.2) When the zero-profit or optimal number of launches exceeds the launch constraint in the projection period, we impose the constraint. If the constraint binds for both the planner and open access firms, then the estimated optimal OUF will be zero. If the constraint binds on open access firms but not on the planner, the optimal OUF will be lower than if the constraint had not bound open access firms. If we impose the constraint when in reality it would not bind, we will underestimate the optimal OUF.

## 1.4 Sensitivity analyses of physical equation calibration

To study the sensitivity of our conclusions to uncertainty in our physical parameter estimates, we conduct a sensitivity analysis of the model simulations given different physical parameter values. We use a residual bootstrap procedure to obtain sets of alternative parameter values.

First, we estimate equations 12 and 13 as described above. Then, we sample from the distribution of residuals to generate "bootstrap worlds". We add these residuals to the estimated models to generate bootstrap world outcome variables. Finally, we re-estimate equations 12 and 13 using the bootstrap world outcomes to generate alternate sets of physical parameter estimates, and simulate the open-access and optimal models under a random sample of those estimates. Algorithm 4 describes our procedure precisely.

One issue to note is that, because we estimate equation 12 with a constrained procedure and the coefficients are near one of the constraint boundaries, the asymptotic properties of our main model estimates are difficult to obtain [14].[19]

---

and are well-suited for cases where the data are obtained from non-uniformly distributed sites. In the two-dimensional case used here, thin-plate splines arise as minimizers of the following objective function with $n$ observations, $y_i$ being the outcomes, and $(S,D)_i$ being the predictors:

$$E(f) = \sum_{i=1}^{n} ||y_i - f((S,D)_i)||_2^2 + \lambda \int\int ||\mathbf{H}f||_2^2 dSdD,$$

where $\mathbf{H}f$ is the matrix of second-order partial derivatives of $f$, and $||\cdot||_2^2$ is the sum of squares of the argument (squared $L_2$-norm). Thin-plate splines can be interpreted by physical analogy as bending a thin plate of metal to fit an underlying surface without allowing it to move at the sample points. In two dimensions, the $\lambda \int\int ||\mathbf{H}f||_2^2 dSdD$ term can be viewed as the bending energy of the plate. The objective function therefore balances the goodness-of-fit (the first term in the objective function) against the amount of bending energy (the second term). We choose the penalty parameter $\lambda$ by cross-validation. Thin-plate splines are a convenient multidimensional interpolator here because they are infinitely differentiable and preserve shape properties of the underlying function. For more the use of on shape-preserving methods in economic dynamic programming problems, see [4].

[19] The issues described in [14] make straightforward sampling from the estimated covariance matrix inappropriate for our setting. This would motivate a non-parametric approach, but our small sample size precludes fully non-parametric bootstrapping. We opt for a semi-parametric procedure

**Algorithm 4:** Bootstrap procedure

1 Estimate equations 12 and 13 to obtain base parameter estimates, $\Phi$, and residuals, $\{(\varepsilon_{Lt}, \varepsilon_{Dt})\}_t$.
2 Draw from $\{(\varepsilon_{Lt}, \varepsilon_{Dt})\}_t$ with replacement to generate $b = 1, \ldots, B$ bootstrap resamples $\{(\varepsilon_{Lt}, \varepsilon_{Dt})^b\}_t$.
3 Generate $B$ bootstrap time series, $L^b(S_t, D_t)$ and $D^b_{t+1}$, using equations 12 and 13 with base estimates $\Phi$ and resampled residuals $\{(\varepsilon_{Lt}, \varepsilon_{Dt})^b\}_t$.
4 Re-estimate equations 12 and 13 using $L^b(S_t, D_t)$ and $D^b_{t+1}$ as dependent variables to obtain bootstrap parameter estimates $\{\Phi^b\}_1^B$.

## 1.5 Projecting the optimal OUF path

With the calibrated parameter values, we turn to projecting the optimal OUF path. We split this process into two stages. In the first stage, we compute the time paths of the satellite stock, debris stock, and launch rate, given the open access and fleet planner models of orbit use. These describe the projected evolution of the orbital aggregates. In the second stage, we use the computed time paths with the estimated collision probability function and launch cost path to calculate the optimal OUF. The OUF is derived from the same open access and fleet planner models. It describes the amount which a satellite owner would have to be charged every year, beginning from the projection horizon's initial conditions, in order to align their incentives with the fleet planner's.[20] We show the in-sample fit of our open access projections to establish that our approach can approximate the observed history, and then use predictions of space economy revenues and costs from Jonas et al. [12] to project out the open access and optimal launch rates given those predictions.

We calculate the time path of an optimal OUF from equation 16. Letting $X^o_t$ denote the open-access launch rate in period $t$, $X^*_t$ denote the optimal launch rate in period $t$, and $\tau_t$ denote the optimal OUF,

$$\tau_t : X^o_t = X^*_t.$$

In general, the optimal Pigouvian tax on a variable is the marginal external cost of that variable. For satellites being launched in period $t$, this means

$$\tau_t = \xi(S^*_{t+1}, D^*_{t+1}).$$

The equilibrium and optimal relationships from equations 7 and 9 offer a convenient way to compute the marginal external cost from the observable collision probability under open access and the counterfactual collision probability under optimal management:

$$\begin{aligned} L(S^*_{t+1}, D^*_{t+1}) &= 1 + r_{s,t+1} - (1+r)\frac{F_t}{F_{t+1}} - \xi(S^*_{t+1}, D^*_{t+1}) \\ L(S^o_{t+1}, D^o_{t+1}) &= 1 + r_{s,t+1} - (1+r)\frac{F_t}{F_{t+1}} \\ \implies \tau_t &= (L(S^o_{t+1}, D^o_{t+1}) - L(S^*_{t+1}, D^*_{t+1}))F_{t+1}, \end{aligned} \tag{16}$$

where $S^o_{t+1}$ and $D^o_{t+1}$ are satellite and debris stocks in $t+1$ under open access management, and $S^*_{t+1}$ and $D^*_{t+1}$ are satellite and debris stocks in $t+1$ under optimal management. The difference in collision probabilities provides a dimensionless "rate" of marginal external cost, so re-scaling the rate by $F_{t+1}$ converts the rate back into the appropriate monetary units. After the initial period of optimal management, the optimal trajectories of satellite and debris stocks diverges from the open-access trajectories. The OUF reflects the additional rents accruing to satellite owners because of management, which would be dissipate under open access.

As we stated earlier, the optimal OUF is the marginal external cost of launching another satellite. As such, it is positive whenever the planner would maintain a lower collision probability than firms under open access would. The planner, in turn, will maintain a lower collision probability if the lifetime returns from another satellite in orbit are

to split this difference and account for our model structure without imposing overly-restrictive conditions on the asymptotic coefficient distributions. The residual bootstrap is a particular semi-parametric bootstrap method developed for AR(1) models, making it more appropriate for equation 13 [16].

[20] This can also be thought of as "How much of the profits from orbit use currently reflect resource rents which should not have been dissipated?"

less than that satellite's expected future damages to other satellites in the fleet. By charging open access firms the marginal external cost of their satellite as an OUF, their incentives are aligned with those of the planner despite the institutional differences. With their incentives aligned, their decisions to launch or not are shifted to optimize the total intertemporal economic value from orbit use rather than their own individual profit.

Formally, equation 16 can be derived by comparing the open access equilibrium condition (equation 7) to the fleet planner's optimality condition for launching (the first-order condition of system of equations 8).[21] These conditions can be written to express the expected loss in satellite value (collision probability multiplied by replacement cost) in terms of economic and, in the case of the optimality condition, physical parameters. Those economic parameters include terms for the current excess return on a satellite in addition to the capital gain or loss from changes in the cost of a replacement satellite. By subtracting the optimal expected collision probability from the open-access expected collision probability, we recover the additional physical and economic term the fleet planner accounts for—the marginal external cost of a satellite. The marginal external cost is the optimal OUF value to levy on each satellite.

## 1.6 Projecting the effects of active debris removal under open access

Finally, we consider the effects of active debris removal technologies on the NPV losses due to open access, shown in Figure 4 of the main text. We assume that debris removal is available for zero cost, and that 50% of all debris is removed from orbit each period once the technology is available. For example, in a scenario where removal begins in 2030, we assume that 50% of all debris in orbit is removed every year beginning in 2030. We assume debris is removed before it collides with any other orbiting object, and that implementing the removal technology does not require any additional satellites.

These assumptions help us bound a "best case" removal scenario. In reality, removal will cost more than $0 per unit removed, will require some additional satellites on orbit to implement, and will not be guaranteed to be successful in all cases. Since debris removal in LEO is not commercially available yet, we experiment with different removal start years between 2021–2034.

The laws of motion with debris removal are

$$S_{t+1} = S_t(1 - L(S_t, D_t(1-R_t)))\mu + X_t \tag{17}$$
$$D_{t+1} = D_t(1-R_t)(1-\delta) + G(S_t, D_t(1-R_t)) + \gamma A_t + mX_t, \tag{18}$$

where $R_t = 0.5$ if removal technologies are available and 0 otherwise.

The open access equilibrium condition is unchanged from the condition without debris removal(equation 7). The planner's optimality condition with freely-provided debris removal is similar to the condition without debris removal (equation 9), but with $(1-R_t)$ terms scaling the debris variable and all derivatives with respect to debris:

$$\begin{aligned} W_{D,t}(S_t, D_t(1-R_t)) = &- S_t L_D(S_t, D_t(1-R_t))(1-R_t)F_t + \\ &\beta[1 - \delta + G_D(S_t, D_t(1-R_t))(1-R_t) + \\ &mS_t L_D(S_t, D_t(1-R_t))(1-R_t)]W_{D,t+1}(S_{t+1}, D_{t+1}(1-R_{t+1})), \end{aligned} \tag{19}$$

[21] The traditional way to calculate the marginal external cost of another launch in this setting would be to derive the marginal value of a satellite ($W_S$) and the marginal value of debris ($W_D$), then determine which (if any) of those marginal values were already being internalized by firms, then assess the remainder on firms as a fee. The calculation in equation 16 implements this calculation, but is more convenient in that it allows us to do a simple comparison of observable variables rather than calculate the derivatives of the planner's value function and the open-access fleet value and take differences.

where

$$W_{D,t}(S_t, D_t(1-R_t)) = \Bigg[\frac{F_{t-1}}{\beta} - \pi_t - (1 - L(S_t, D_t(1-R_t)) - S_t L_S(S_t, D_t(1-R_t)))F_t - \left(\frac{G_S(S_t, D_t(1-R_t)) - m(1 - L(S_t, D_t(1-R_t)) - S_t L_S(S_t, D_t(1-R_t)))}{1 - \delta + G_D(S_t, D_t(1-R_t))(1-R_t) + mL_D(S_t, D_t(1-R_t))(1-R_t)}\right) \cdot L_D(S_t, D_t(1-R_t))(1-R_t)S_t F_t\Bigg] \cdot \left[\frac{G_S(S_t, D_t(1-R_t)) - m(1 - L(S_t, D_t(1-R_t)) - S_t L_S(S_t, D_t(1-R_t)))}{1 - \delta + G_D(S_t, D_t(1-R_t))(1-R_t) + mL_D(S_t, D_t(1-R_t))(1-R_t)} + m\right]^{-1}. \tag{20}$$

## 1.7 Derivation of the open-access launch rate

In this section we derive equations characterizing the interior open-access launch rate under constant and time-varying parameters and infinite lifetimes, equations 6 and 7.[22] These results are shown in [21], and included here for interested readers. We begin with the case where parameters are constant over time, equation 6.

A firm, $i$, deciding whether to launch or not solves

$$\begin{aligned} V_i(S_t, D_t, X_t) &= \max_{x_{it} \in \{0,1\}} \{(1 - x_{it})\beta V_i(S_{t+1}, D_{t+1}, X_{t+1}) + x_{it}[\beta Q(S_{t+1}, D_{t+1}, X_{t+1}) - F]\} \\ \text{s.t. } S_{t+1} &= S_t(1 - L(S_t, D_t)) + X_t \\ D_{t+1} &= D_t(1-\delta) + G(S_t, D_t) + \gamma A_t + mX_t, \end{aligned}$$

with the value of a satellite being

$$Q(S_t, D_t, X_t) = \pi + \beta(1 - L(S_t, D_t))Q(S_{t+1}, D_{t+1}, X_{t+1}). \tag{21}$$

In an open-access equilibrium, firms are indifferent between launching or not launching because the profits from owning a satellite have been driven to zero. This gives us the following:

$$\begin{aligned} X_t \in [0, \bar{X}] :\ V_i(S_t, D_t, X_t) &= 0 && (22)\\ \implies \beta Q(S_{t+1}, D_{t+1}, X_{t+1}) &= F && (23)\\ \implies Q(S_t, D_t, X_t) &= \pi + (1 - L(S_t, D_t))F && (24)\\ \implies \pi &= rF + L(S_{t+1}, D_{t+1})F && (25)\\ \implies L(S_{t+1}, D_{t+1})F &= \pi - rF && (26)\\ \implies L(S_{t+1}, D_{t+1}) &= r_s - r. && (27) \end{aligned}$$

Equation 25 follows from substituting equation 24 into equation 21. Equation 26 follows from iterating equation 25 one period forward and and substituting it into equation 24. The final line (which is equation 6) follows from the definition $r_s \equiv \pi/F$, with the right-hand side being defined as the excess return on a satellite.

Note that equation 6 does not imply a constant launch rate or a steady state in orbit. Any pattern of dynamics such that equation 6 holds is consistent with an open-access equilibrium. Such patterns include paths where the satellite stock is increasing while the debris stock is decreasing, or paths where the satellite stock is decreasing while the debris stock is increasing. While the system defined by equations 6, 2, and 3 will eventually converge to an attracting fixed point in $(S, D)$ space whenever such a fixed point exists, the dynamics of the system will be governed by the properties of $L$ and $G$. While our calibrations ensure the existence of a unique stable steady state, such properties are not guaranteed in systems where Kessler Syndrome is possible.

[22] Including finite lifetimes scales the collision risk by the probability of natural satellite end-of-life occurring, but does not change any qualitative properties.

The derivation of equation 7 follows much as the derivation of equation 6. Beginning from the same equilibrium condition and net present value of a satellite (both value functions augmented with time subscripts), and allowing $\pi$ and $F$ to vary over time,

$$X_t \in [0,\bar{X}]: \; V_{it}(S_t,D_t,X_t) = 0 \tag{28}$$
$$\implies \beta Q_{t+1}(S_{t+1},D_{t+1},X_{t+1}) = F_t \tag{29}$$
$$\implies Q_t(S_t,D_t,X_t) = \pi_t + (1-L(S_t,D_t))F_t \tag{30}$$
$$\implies \pi_{t+1} = (1+r)F_t + L(S_{t+1},D_{t+1})F_{t+1} \tag{31}$$
$$\implies L(S_{t+1},D_{t+1}) = 1 + \frac{\pi_{t+1} - (1+r_t)F_t}{F_{t+1}} \tag{32}$$
$$\implies L(S_{t+1},D_{t+1}) = \left(r_{s,t+1} - r\frac{F_t}{F_{t+1}}\right) + \left(1 - \frac{F_t}{F_{t+1}}\right). \tag{33}$$

Note that giving firms the option to deorbit a satellite does not affect the equilibrium collision probability. To see this, consider a firm which owns a satellite and must decide whether or not to deorbit it. Let $V_t^d$ denote the net payoff from deorbiting a satellite. $V_t^d$ includes any liquidation revenues or costs from deorbiting, e.g. revenues from selling equipment or costs incurred due to service disruptions, and may be positive, negative, or zero. At the beginning of a period, satellite-owning firms decide whether to keep their satellite operational and collect revenues, or deorbit the satellite.

The ability of a satellite owner to deorbit does not change the problem facing an open-access launcher, so equation 30 still characterizes the continuation value of owning a satellite. Under open access, the satellite-owning firm solves

$$Q_t(S_t,D_t,X_t) = \max\{\pi_t + (1-L(S_t,D_t))F_t, V_t^d\}. \tag{34}$$

This implies a satellite-owning firm will deorbit their satellite in $t$ if

$$V_t^d > \pi_t + (1-L(S_t,D_t))F_t \tag{35}$$
$$L(S_t,D_t) > 1 + \frac{\pi_t - V_t^d}{F_t}. \tag{36}$$

Since $L$ is a probability and bounded in $[0,1]$, as long as the satellite is expected to produce more profit in $t$ than can be obtained by deorbiting it a firm will never choose to deorbit it. Even if $V_t^d > \pi_t$, it may still be more profitable to leave it in orbit if the collision risk is sufficiently low that the expected continuation value of leaving the satellite in orbit exceeds the returns to deorbiting it.

Since we do not observe $V^d$ in our data, we simply assume a constant fraction $\mu$ of satellite owners choose to deorbit their satellites each period and calibrate that fraction to the data.

## 1.8 Derivation of the optimal launch rate

In this section we derive the equations characterizing the planner's interior launch rule, equations 9 and 10. Period $t$ values are shown with no subscript, and period $t+1$ values are marked with a $'$, e.g. $S_t \equiv S, S_{t+1} \equiv S'$. The fleet planner's problem is

$$W(S,D) = \max_{X\geq 0}\{\pi S - FX + \beta W(S',D')\} \tag{37}$$
$$\text{s.t. } S' = S(1-L(S,D))\mu + X \tag{38}$$
$$D' = D(1-\delta) + G(S,D) + \gamma A + mX. \tag{39}$$

The fleet planner's launch plan will satisfy

$$X^*: \beta[W_S(S',D') + mW_D(S',D')] = F, \tag{40}$$

that is, the planner will launch until the marginal value to the fleet of a new satellite plus the marginal value to the fleet of its launch debris is equal to the launch cost.

Assuming an optimal policy function $X^* = H(S,D)$ exists and applying the envelope condition, we have the following expressions for the fleet's marginal value of another satellite and another piece of debris:

$$W_S(S,D) = \pi + \beta[W_S(S',D')(1 - L(S,D) - SL_S(S,D))\mu + W_D(S',D')G_S(S,D)] \tag{41}$$
$$W_D(S,D) = \beta[W_D(S',D')(1 - \delta + G_D(S,D)) + W_S(S',D')(-SL_D(S,D)\mu)] \tag{42}$$

Rewriting equation 40, we have

$$W_S(S',D') = \left[\frac{F}{\beta} - mW_D(S',D')\right] \tag{43}$$

Plugging equation 43 into equations 41 and 42,

$$W_S(S,D) = \pi + F(1 - L(S,D) - SL_S(S,D))\mu - \beta W_D(S',D')[m(1 - L(S,D) - SL_S(S,D)\mu) - G_S(S,D)] \tag{44}$$
$$W_D(S,D) = (-SL_D(S,D))F + \beta W_D(S',D')[1 - \delta + G_D(S,D) - m(-SL_D(S,D)\mu)] \tag{45}$$

Define the following quantities:

$$\alpha_1(S,D) = \pi + (1 - L(S,D) - SL_S(S,D))\mu F$$
$$\alpha_2(S,D) = -SL_D(S,D)\mu F$$
$$\Gamma_1(S,D) = G_S(S,D) - m(1 - L(S,D) - SL_S(S,D))\mu$$
$$\Gamma_2(S,D) = 1 - \delta + G_D(S,D) + mSL_D(S,D)\mu.$$

These allow us to rewrite equations 44 and 45 as

$$W_S(S,D) = \alpha_1(S,D) + \beta\Gamma_1(S,D)W_D(S',D') \tag{46}$$
$$W_D(S,D) = \alpha_2(S,D) + \beta\Gamma_2(S,D)W_D(S',D'). \tag{47}$$

As long as $\delta < 1$, $\Gamma_2(S,D) \neq 0 \; \forall (S,D)$, allowing us to rewrite equation 47 as

$$W_D(S',D') = \frac{W_D(S,D) - \alpha_2(S,D)}{\beta\Gamma_2(S,D)}. \tag{48}$$

Plugging equation 48 into equation 46, we get

$$\begin{aligned} W_S(S,D) &= \alpha_1(S,D) + \beta\Gamma_1(S,D)\frac{W_D(S,D) - \alpha_2(S,D)}{\beta\Gamma_2(S,D)} \\ &= \alpha_1(S,D) + \frac{\Gamma_1(S,D)}{\Gamma_2(S,D)}(W_D(S,D) - \alpha_2(S,D)) \\ \implies W_S(S,D) &= \alpha_1(S,D) - \frac{\Gamma_1(S,D)}{\Gamma_2(S,D)}\alpha_2(S,D) + \frac{\Gamma_1(S,D)}{\Gamma_2(S,D)}W_D(S,D) \end{aligned} \tag{49}$$

Iterating equation 43 one period backwards and plugging it into equation 48, we get

$$\begin{aligned} \frac{'F}{\beta} - mW_D(S,D) &= \alpha_1(S,D) - \frac{\Gamma_1(S,D)}{\Gamma_2(S,D)}\alpha_2(S,D) + \frac{\Gamma_1(S,D)}{\Gamma_2(S,D)}W_D(S,D) \\ \implies W_D(S,D) &= \left[\frac{'F}{\beta} - \alpha_1(S,D) - \frac{\Gamma_1(S,D)}{\Gamma_2(S,D)}\alpha_2(S,D)\right]\left[\frac{\Gamma_1(S,D)}{\Gamma_2(S,D)} + m\right]^{-1}. \end{aligned} \tag{50}$$

Substituting in the forms for $\alpha_1(S,D), \alpha_2(S,D), \Gamma_1(S,D)$, and $\Gamma_2(S,D)$, equation 50 yields

$$\begin{aligned} W_D(S,D) = &\left[\frac{'F}{\beta} - \pi - (1 - L(S,D) - SL_S(S,D))\mu F - \frac{G_S(S,D) - m(1 - L(S,D) - SL_S(S,D))\mu}{1 - \delta + G_D(S,D) + mL_D(S,D)\mu}L_D(S,D)\mu SF\right] \cdot \\ &\left[\frac{G_S(S,D) - m(1 - L(S,D) - SL_S(S,D))\mu}{1 - \delta + G_D(S,D) + mL_D(S,D)\mu} + m\right]^{-1}. \end{aligned} \tag{51}$$

Combining equation 51 with equation 50 iterated one period forwards, we obtain

$$L(S',D') = 1 + r'_s - (1+r)\frac{F}{F'} - \xi(S',D'),$$

where

$$\xi(S',D') = S'L_S(S',D')\mu F' + \frac{\pi - rF - L(S,D)\mu F - SL_S(S,D)\mu F}{\beta(1-\delta+G_D(S',D')+mL_D(S',D')\mu S')}$$
$$- \frac{\beta G_S(S',D') + m(1-L(S',D') - S'L_S(S',D'))\mu}{\beta(1-\delta+G_D(S',D')+mL_D(S',D')\mu S')} L_D(S',D')\mu S'F'.$$

## 1.9 Discussion

### 1.9.1 Interpreting the optimal OUF and long-run industry value paths

Figure 2 in the main text shows the NPV gains from beginning optimal management in different years, and the permanent orbit use value losses in 2040 from delaying optimal management. The permanent orbit use value is the discounted value of the satellite fleet over the long-run, accounting for losses and replacements.

As mentioned in the main text, the discontinuous jumps in NPV in Figure 2 reflect the immediate effect of reducing launch activity while the satellite and debris stocks are suboptimally high. The change in launch activity increases the NPV by reducing the cost outflows each year. Since open access launching results in excess satellites and debris, the benefits of optimal management continue to accrue gradually as the satellite and debris stocks draw down. Figure 3 in the main text shows these launch rate dynamics for a 2006 optimal management start.

The fact that the optimal OUF, shown in Figure 2 of the main text, rises over time is an indication of the restored value of orbit use due to optimal management (orbital rents). Intuitively, firms fully dissipate orbital rents in an open access equilibrium, as those rents act as an incentive to enter. To counter the growth in the incentive to enter due to restored orbital rents, the OUF must also rise over time. A firm which enters the commons early on (say, 2020) will pay a lower initial fee than a firm which enters later on (say, 2030) because the early entrant is paying to use a more congested environment.

Though our modeling procedure abstracts from many economic and physical complications, our optimal OUF and long-run industry value estimates are likely robust to these limitations and on the correct order of magnitude with the correct qualitative features. On the OUF side, given that the projected optimal launch path beginning from the projected 2020 state of LEO involves cessation of launch activity, the estimated OUF in 2020 needs only to be large enough to deter launches, particularly those likely to generate large and suboptimal increases in collision risk. While satellite operators in LEO are heterogeneous and represent diverse interests, we estimate an optimal averaged-across-LEO-use-cases per-satellite-year fee beginning at approximately $14,849 USD (0.7% of the average annual profits of owning a satellite in 2015) and growing over time. [17] identify that the majority of collision risk increases in the near future will be driven by satellite constellation operators. For an entity planning to launch a constellation of 600 satellites, our OUF amounts to an additional yearly expenditure beginning at roughly $8.91 million USD—likely enough to prompt serious reconsideration of the size and nature of the constellation. On the industry value side, the global satellite sector currently produces approximately $0.15 trillion USD in revenues, and is anticipated to grow to $2 trillion USD in revenues and costs by 2040 [12]. A decrease in collision risk which leads to a 10% increase in the per-year economic value of the satellite sector would immediately add 10% to the sector's NPV. Our model projects that collision risk in 2040 will decrease by roughly 33% (compared to BAU) under an optimal management plan beginning in 2020. This reduction in collision risk would cut collision-related replacement costs, increase the expected lifespan of satellites in orbit, and reduce collision-related disruptions in the stream of satellite-related economic returns. Given this, long-run industry value in 2040 on the order of single-digit trillions of USD seems plausible.

### 1.9.2 Open access and active debris removal

The introduction of debris removal makes both open access firms and the planner launch additional satellites. However, the planner launches considerably fewer additional satellites than open access firms. The immediate decrease in

debris when removal becomes available induces new launches under open access until the collision risk is once again equated with the excess return on a satellite. Figure 4 of the main text shows the effects of debris removal beginning in 2029 on satellite and debris accumulation under open access and a range of optimal management paths. The removal-induced additional launching leads to a higher steady-state satellite stock and a lower steady-state debris stock under open access and optimal management. The amount of debris removed in our "50% removal" scenario is substantially larger under open access than the optimal plan as there is more debris in orbit under open access.

Though debris removal allows open access to sustain more satellites in orbit, over time collision risk returns to the equilibrium level. The costs of additional launches erodes some of the NPV gains due to reduced risk. Figure 4e in the main text shows the percentage change in open-access NPV loss due to the introduction of debris removal in 2029, as a fraction of the potential gain from implementing the optimal plan in 2020. Figure 4f in the main text summarizes the minimum, mean, and maximum changes in long-run industry value losses due to open access with removal beginning in each year in 2021–2034. On average, debris removal beginning in the 2021–2034 window reduces open access NPV losses by about 1.74% relative to a counterfactual world without removal. When optimal management begins ahead of debris removal, the NPV losses tend to be reduced (negative changes). When optimal management begins after debris removal, the NPV losses tend to be increased (positive changes). The increase in NPV losses in the latter scenario is driven by the costs of additional launching under open access, both immediately following the initial debris reduction and to sustain the larger satellite population. Due to open access, firms will take advantage of lower collision risk due to debris removal by launching satellites until there are no more profits from launching new satellites. When the planner is in charge of launching before debris removal begins, they do not waste resources by launching to dissipate the gains from debris removal.

Eventually, it seems likely that debris removal will become technologically feasible at a unit price low enough to be economically viable (but greater than the zero dollars we consider here). Some existing studies which have estimated bounds on willingness-to-pay for debris removal, highlighted strategic issues in debris removal which threaten to limit the value of a removal industry, suggested financing mechanisms, or detailed the legal and policy landscape [19, 15, 5, 23, 1]. There are many more interesting questions about the as-yet nonexistent debris removal industry. Should it be private? Public? How should it be funded? The OUF we calculate is not the marginal willingness-to-pay for debris removal, and does not provide guidance on the potential value or structure of a future debris removal industry.[23] These questions are important for future research to address in detail.

### 1.9.3 Unmodeled physical and economic factors

In addition to the limitations imposed by modeling spatially and temporally heterogeneous physical and economic processes at an aggregated level, there are three main analytical limitations pertaining to unobservables in the past and present and unknowables in the future: launch market frictions, constellations (coordinated systems of satellites intended to serve a common purpose), and satellite placement. These limitations may make our OUF estimates lower bounds on the true values required to induce optimal orbit use, as we describe below.

Our conclusions about the suboptimality of open access to orbit and the necessity of a globally-coordinated OUF (or policies equivalent to one) are robust to these limitations. The fundamental problem creating the need for policies equivalent to a globally-coordinated OUF is the lack of legally-enforceable property rights over orbits.[24] The lack of property rights prevents satellite owners from internalizing the costs they impose on others through collision risk and debris creation. The same issue manifests in other common-resource settings, such as fisheries [9].

Our economic model is founded on the assumption that all agents who want to launch satellites are able to do so with no frictions. In practice, there are factors other than orbital property rights and willingness-to-pay which limit agents' access to orbit, such as limited availability of launch windows and rockets. These factors constrain humanity's ability to launch satellites. To ensure that our simulations do not violate this launch constraint in observed years, we

[23] The OUF is the marginal external cost of another satellite at the optimum, accounting for that satellite's dynamic effect on collision risk through debris and other satellites. It is not the marginal external cost of another piece of debris at the optimum, as the external cost of another satellite entering orbit is not the same as the external cost from another piece of debris. This is related to the point on lines 269-273 of the main text about computing an OUF for a 'standard unit' of risk—active satellites and debris would not generate the same number of standard units of risk.

[24] The geostationary belt is the exception to this statement. In general, however, there is no globally-coordinated procedure for allocating orbital paths, or even a globally-agreed-upon definition of an orbital path property right.

calculate the launch constraint in each observed period as the cumulative maximum number of launches observed so far. The shadow value of the launch constraint is recovered in the economic parameter calibration process, but the individual factors are not identifiable from the data. We then fit a linear time trend to the observed launch constraint, and project it into the future. To the extent that the launch constraint will be relaxed faster than a linear trend would predict, our estimates are economically conservative, i.e. we assume fewer launches than may occur, which biases our estimated OUF downward.

Our economic model is also founded on the simplifying assumption of "one satellite per firm".[25] In practice, there are a number of firms which own constellations or fleets of satellites. However, unless a single firm owned all satellites in orbit, orbit users would not internalize the full scope of the externality they impose on others. To the extent that the observed data reflects agents internalizing those externalities due to ownership of multiple satellites, our economic parameter estimates would entangle those factors with the estimated launch constraint shadow value. Our projections of single-satellite-owning firms' responses to increases in satellite profitability would therefore be attenuated toward zero, making our projections environmentally conservative, i.e. closer to an environmental "worst-case" analysis. However, the same assumption also increases the optimal OUF we estimate.

Lastly, our model abstracts away entirely from the question of satellite placement. That is, two orbital objects within a given volume shell can be placed in orbits such that at one extreme they are guaranteed to collide, or at the other extreme they will never collide. Our projections are based on collision rate estimates which are calculated using historical placement patterns. Thus, our projections assume that the systematic factors which resulted in current object placements will continue into the future. While technology and constellation ownership are likely to lead to improvements in placement patterns our collision risk projections would be biased for both the open access and optimal launch paths. However, the magnitude of the gap between open access and optimal collision risk may actually be understated by this issue. To the extent that economic agents have the placement margin available to them it is induces another externality, similar in spirit but different in detail to the orbit use externality we describe in this article, wherein firms do not account for the full magnitude of orbital-use efficiency losses due to their placement. A fleet planner who coordinated all satellites in orbit would account for such placement-related externalities. By taking advantage of any efficiencies in placement, the planner would be able to reduce collision rates below what open access satellite owners would have an incentive to consider. Thus, while the inclusion of a placement margin may reduce levels of collision risk, the differences in collision risk between open access and optimal use may increase or decrease. If the differences in collision risk increased, our OUF estimates would be a lower bound on average.[26]

### 1.9.4 Collision avoidance by active satellites

The 1972 Convention on International Liability for Damage Caused by Space Objects ("Liability Convention") states that the entity which launched a satellite holds liability for any damage done by one satellite to other satellites. While the Liability Convention has yet to be tested at scale (leaving many open questions about attribution and enforcement, as discussed in the main text), it is reasonable to argue that satellite operators will make efforts above and beyond simply protecting their assets to avoid collisions between their satellites and other objects. Launchers of new mega-constellations are increasingly launching smaller satellites, and equipping them with sophisticated automated collision avoidance protocols. While these technological shifts are quite different from increased clarity around and enforcement of the Liability Convention, they are similar in reducing the probability of collision between active satellites and other entities below what a purely statistical model might predict.

Detailed models of how these factors might affect the collision risk and other equilibrium outcomes are beyond our scope in this article. To consider how they might affect equilibrium outcomes and the optimal OUF, we conduct a simple counterfactual exercise. We cut the physical collision probability parameters $\alpha_{SS}$ and $\alpha_{SD}$ in half from their estimated values, reflecting that the actual physical collision rates may be substantially lower than a statistical model's predictions, and simulate the model forward from 2006. We then plot the time paths of open access and optimal management launches, satellite and debris stocks, collision risk, as well as the relative advantage of optimal management

[25] Our assumption could be relaxed to assuming that only the marginal firm launching owns one satellite and would still yield the same equilibrium condition. Since we are abstracting from firm heterogeneity, we do not apply this interpretation.

[26] While some regimes in a spatially-differentiated orbit model may have lower OUF values than the ones we calculate here, others may have higher OUF values.

and the OUF, from 2020 onwards. As in our main policy environment analysis, we assume optimal management begins in 2020. Figure S7 shows these results.

Collision avoidance (whether due to liability concerns, smaller satellites, automated avoidance, or any combination) increases both the open access and optimal levels of satellites while reducing the collision probability. The launch rates and debris stocks in this scenario eventually rise above the estimated scenario. The increase in launch rates is to sustain the larger satellite population. The increase in debris stocks is in part due to greater launch debris from those additional launches, and partly due to a larger number of collisions from larger satellite populations. However, collision avoidance in this scenario reduces the consequences of larger debris stocks, meaning the collision probability remains below the non-avoidance scenario levels. The smaller collision probabilities (and smaller gap between open-access and optimal collision probabilities) imply generally lower OUFs. While the OUF in the avoidance scenario begins at roughly the same level as in the non-avoidance scenario, by 2040 it is around 68% the non-avoidance level—approximately \$161,149 (around 7.7% of the annual profits of operating a satellite in 2015) per satellite-year with avoidance, compared to \$234,227 (around 11% of the annual profits of operating a satellite in 2015) per satellite-year without avoidance). Even with collision avoidance, optimal management reflects at least a five-fold increase in NPV relative to open access.

### 1.9.5 Discount rate sensitivity

We assume a 5% discount rate in our analysis. We chose 5% to reflect industry opportunity costs, since the planner we study is an industry fleet manager (the sole owner benchmark used in other natural resource settings). To assess the sensitivity of our conclusions to the chosen discount rate, we simulate the model under discount rates from 3% to 7%. Figure S8 shows these results.

Increasing the discount rate to 7% reduces the relative gain from optimal management to about 3.5 times the BAU open access rate, while cutting the discount to 3% increases the relative gain from optimal management to nearly 10-fold BAU. There are two channels through which the discount rate affects the optimal OUF path. Decreasing the discount rate increases the optimal OUF level by increasing the weight attached to future damages (similar to how the discount rate affects optimal carbon taxes in the climate change context). However, there is also a countervailing channel due to the nature of satellites as investment goods for both firms and the planner. Lower discount rates increase both the open access and fleet planner's target levels of satellites as alternative investment opportunities become more attractive. This effect reduces the level of the optimal OUF, counterbalancing the damages effect. For the parameters we estimate these two effects roughly offset each other, leading to relatively invariant optimal OUF paths across different discount rates.

### 1.9.6 Sensitivity to grid resolution

The projected time paths of variables are relatively insensitive to changes in the satellite-debris grid resolution: increasing the grid resolution from 64 points total (8 points in each dimension) to 900 points total (30 points in each dimension) changes the 2040 OUF and optimal-to-BAU NPV ratio (assuming optimal management begins in 2020) from \$234,226 to \$230,488 and 5.79 to 5.86. The distribution of the NPV ratio in 2040 is more sensitive, with higher-resolution grids shifting the distribution of gains upward and concentrating it—under the 64-point grid the middle 95% of projected NPV ratios is between 4.18 and 6.53, while under the 900-point grid the middle 95% of projected NPV ratios is between 6.05 and 6.81. Under all resolutions simulated, the distribution of optimal-to-BAU NPV in 2040 (assuming management begins in 2020) remains greater than 4. Figure S9 compares model projections under the 64-point and 900-point grids to illustrate the sensitivity. We report numbers from the coarse grid in the main text since it is quicker to compute, which allows us to show more bootstrap replications.

### 1.9.7 Consequences of measurement error in satellite and debris counts

Limitations of sensor technology suggest that the debris counts we use are lower-bound estimates. To the extent that this biases the collision probability and debris counts downward, it will bias the estimated decay rate, collision probability parameters, fragmentation parameters, and launch debris weakly downwards. Since downward bias in the physical parameters makes collisions and missile tests appear to cause less congestion than they actually do, the open

access and optimal launch rates will be inflated.

Downward bias in the collision probability data will bias the economic parameter estimates weakly downwards as well. This will to some degree offset the inflation in the launch rate caused by the physical parameter underestimation, though the exact extent of the offset is not clear.

In general, measurement error in the collision probability data also causes the nonnegativity constraint on the collision probability parameters ($\alpha_{SS}$ and $\alpha_{SD}$) to bind in some bootstrap replications. This causes issues of the type described in [14] in obtaining asymptotic standard errors.

### 1.9.8 Consequences of collision probability model misspecification

We assume that the collision probability model has constant parameters. Changes in patterns of satellite placement, construction, and ownership structures lead to changes over time in the physical primitives reflected in $\alpha_{SS}$ and $\alpha_{SD}$. The "net" convexity or concavity of the time path of the primitives will determine whether the constant approximations over or understate the true time-varying parameters in any period on average. A convex time path—low values initially and high values later on—will be overestimated on average, while a concave time path—high values initially, with slow increases over time—will be underestimated on average.

The misspecification causes two problems with simulation and inference. First, underestimation will inflate launch rate projections and overestimation will deflate them. However, because the misspecification affects both open access and optimal launch rates in the same way, the simulated optimal OUF will not be affected. Second, underestimation may cause the nonnegativity constraint on the collision probability parameters to bind in some bootstrap replications, causing the same types of asymptotic issues as measurement error.

### 1.9.9 Consequences of measurement error in returns and costs

We take the returns and costs of satellite ownership from the data used in Wienzierl [24], which aggregate revenues from all commercial satellites in orbit. By including more than just LEO satellites, the direct returns and costs data overstate the returns to LEO paths. The economic parameter estimates therefore reflect a "LEO share" coefficient on the revenue data between 0 and 1. The LEO share coefficient attenuates the estimates of $a_{L1}$, $a_{L2}$, and $a_{L3}$.

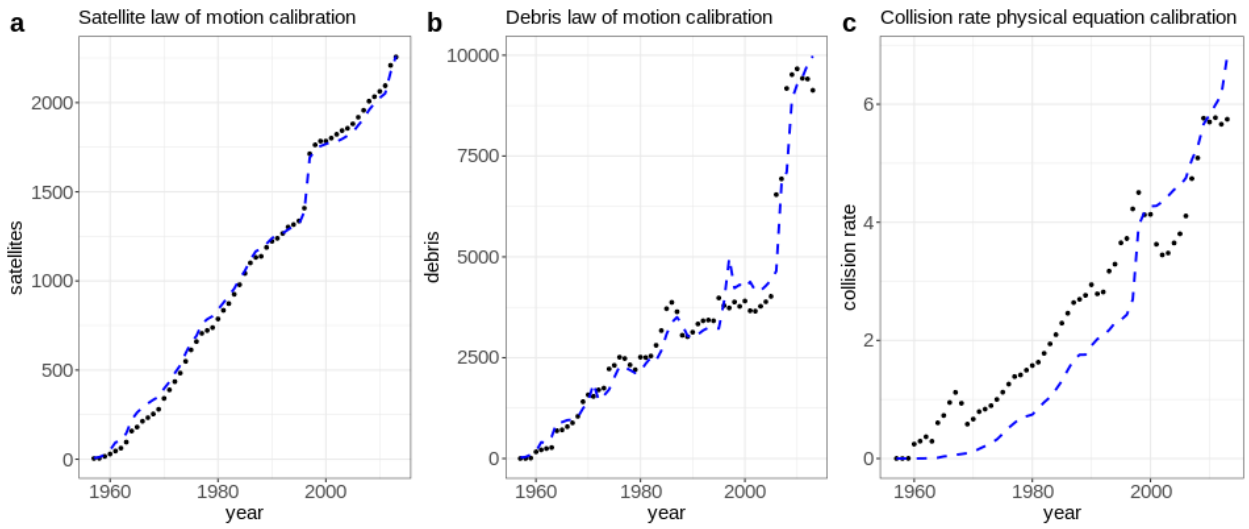


Figure S1: Calibrated physical model fits to historical data. The black dots show historical data points (1957–2014) for debris counts, active satellite counts, and estimated collision rate. The blue dashed lines show the fits of the calibrated models.

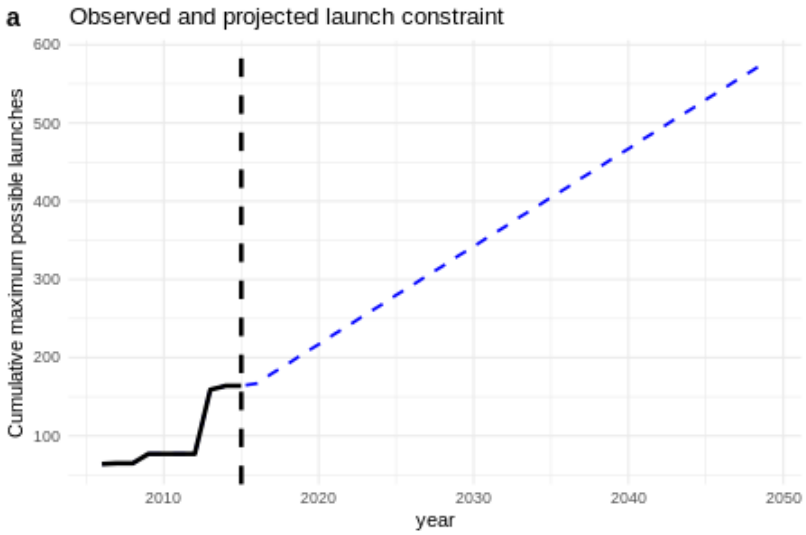


b

| | Estimate | Std. Error |
|---|---|---|
| *Intercept* | 30.13 | 16.43 |
| *Time trend* | 12.5 | 2.65 |

Figure S2: Projected launch constraint model. To represent the various factors constraining the number of rocket launches possible each year – e.g. limited rocket availability, weather-induced launch cancellations, limited launch slots – we model the aggregate launch constraint as a linear time trend based on observed launch behavior from 2006–2015. We use this constraint in our open access and optimal management model simulations to avoid implausibly large launch rates in any given year. Panel a shows the observed and projected launch constraint. The solid black line from 2006–2015 indicates the observed cumulative maximum number of rocket launches in any given year, the dashed blue line from 2016–2050 shows the projected maximum number of rocket launches possible in each year, and the vertical dashed black line marks the end of the in-sample period (2006–2015). Panel b shows the estimated intercept and time trend with standard errors.

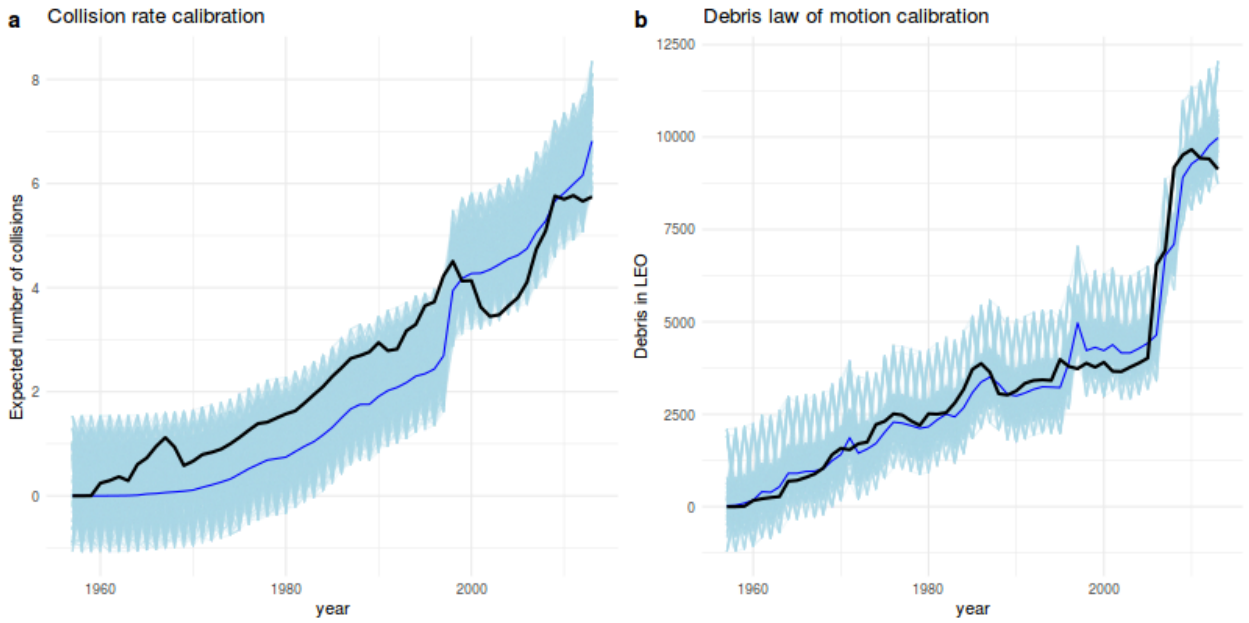


Figure S3: Sensitivity of physical model calibration to parameter uncertainty. Panels a-b show a sensitivity analysis of the model calibrations for the collision rate function and debris law of motion. The black lines show the underlying collision rate and debris count data from ESA, 1957–2014. The thin darker blue lines show the fit of the models calibrated to the black lines (the same model fits shown in figure 3 of the main text). The light blue lines show model fits from residual bootstrap-resampled data, indicating the effects of uncertainty in the model calibration. The same procedure was used to generate Fig. 2d. We describe the residual bootstrap resampling procedure in more detail in section 1.4 of the Supporting Information.

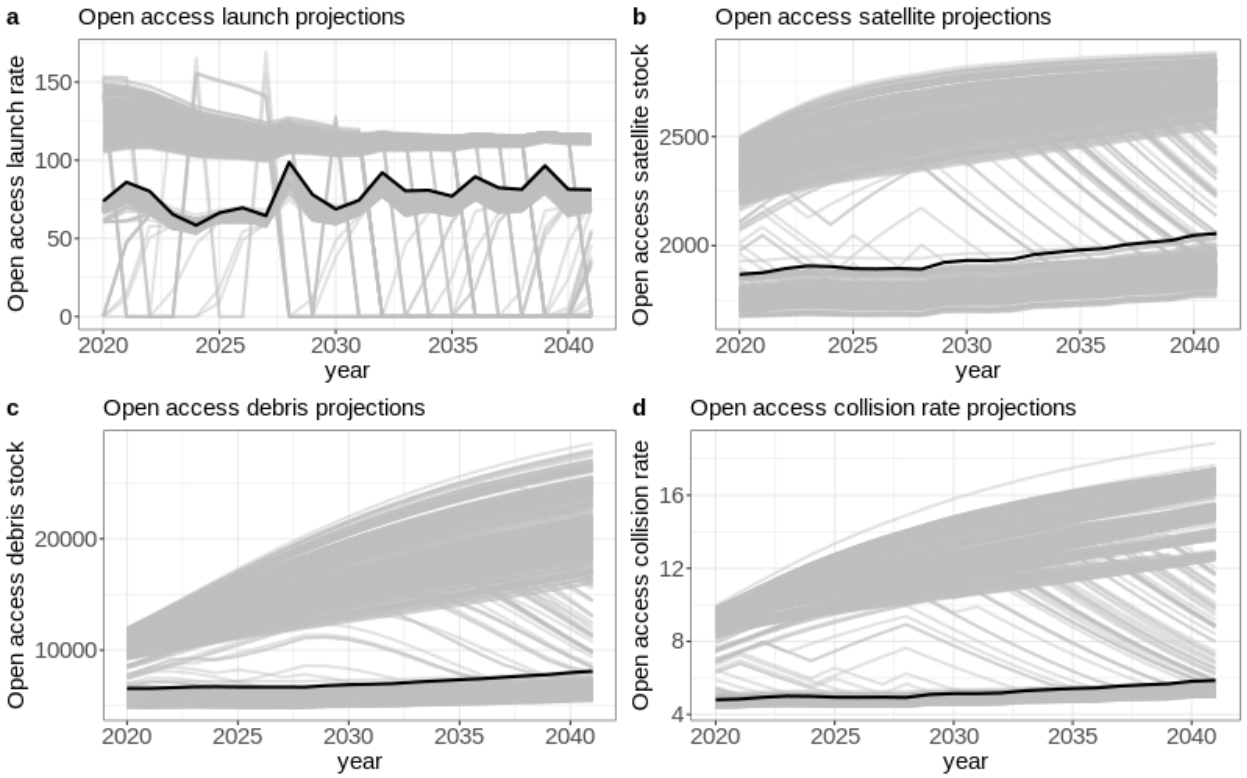


Figure S4: Sensitivity of open-access paths to physical parameter uncertainty. Panels a-d show a sensitivity analysis of open-access model projections beginning in 2020 to uncertainty in the physical parameters. The thick black lines show the projection from the main model estimated on the full 1957–2014 time series of object counts and collision rate estimates. The gray lines show projections using alternate sets of parameter estimates generated from 1000 draws of the residual bootstrap-resampling procedure used in main text figure 2d.

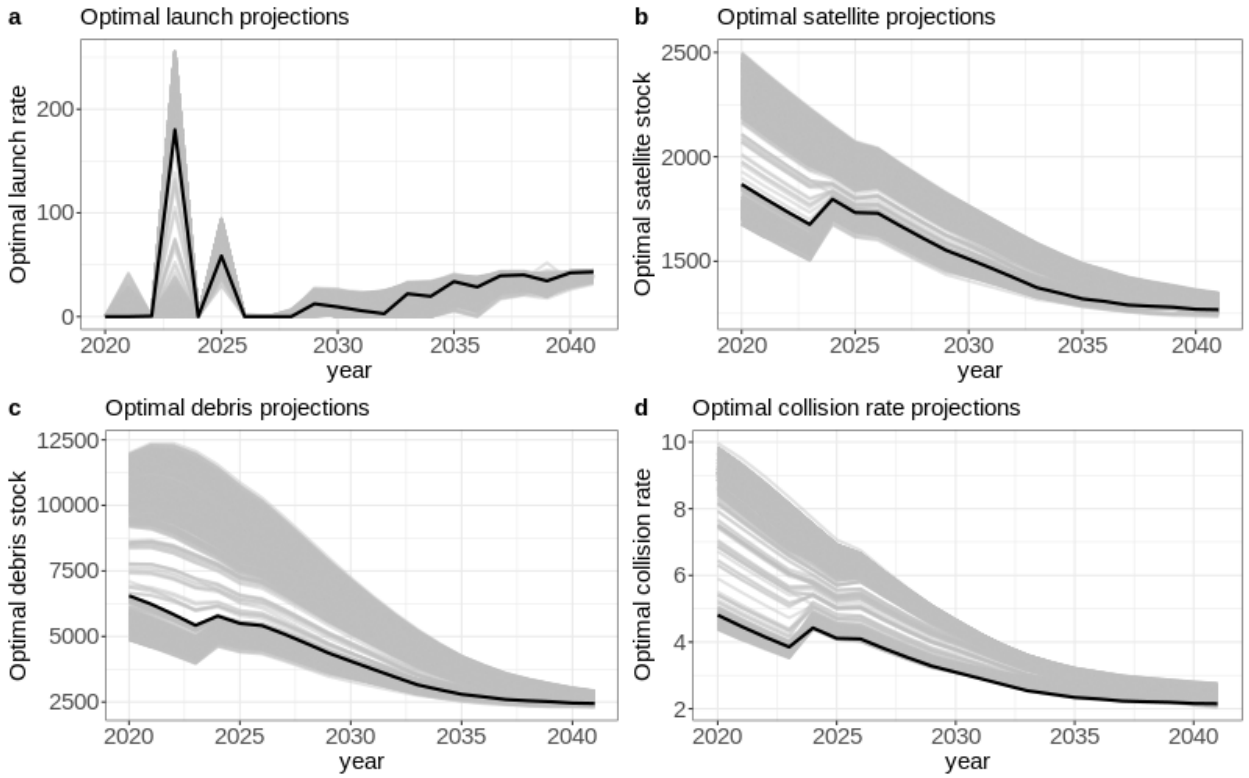


Figure S5: Sensitivity of optimal paths to physical parameter uncertainty. Panels a-d show a sensitivity analysis of optimal model projections beginning in 2020 to uncertainty in the physical parameters. The thick black lines show the projection from the main model, where the physical parameters were estimated on the 1957–2014 calibration time series constructed from ESA and UCS count data. The gray lines show projections using alternate sets of parameter estimates generated from 1000 draws of the residual bootstrap-resampling procedure used in main text figure 2d.

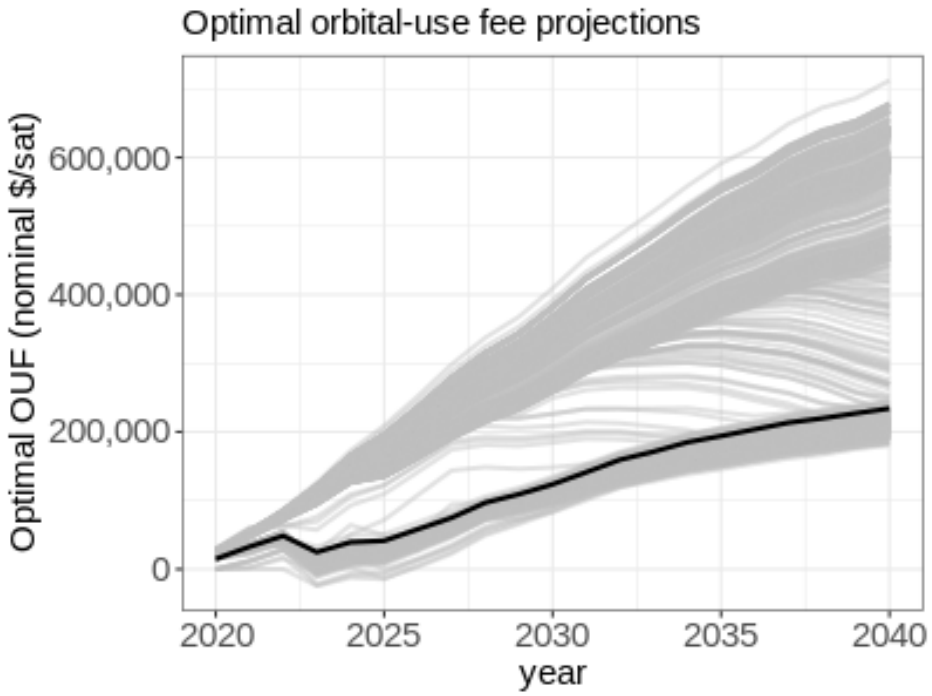


Figure S6: Sensitivity of optimal OUF to physical parameter uncertainty. The thick black line shows the projection from the main model, where the physical parameters were estimated on the 1957–2014 calibration time series constructed from ESA and UCS count data. The gray lines show projections using alternate sets of parameter estimates, generated from 1000 draws of the residual bootstrap-resampling procedure used in main text figure 2d.

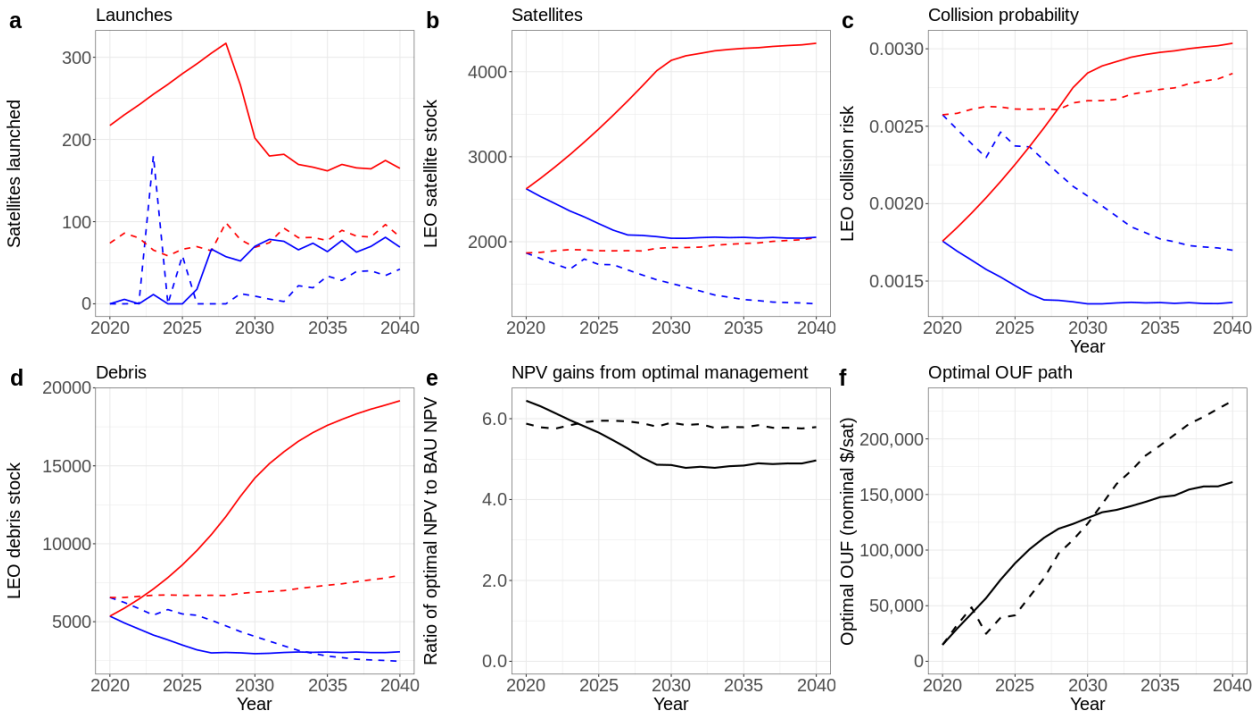


Figure S7: Collision avoidance counterfactual. The dashed lines show model projections with the originally-estimated parameters (i.e. main model estimates from figures S4, S5, and S6), and solid lines show model estimates with the collision-avoidance counterfactual estimates ($\alpha_{SS}$ and $\alpha_{SD}$ half of the estimated values). In panels a-d, the red lines show open-access paths, and the blue lines show optimal management paths beginning in 2020 from the respective open-access levels.

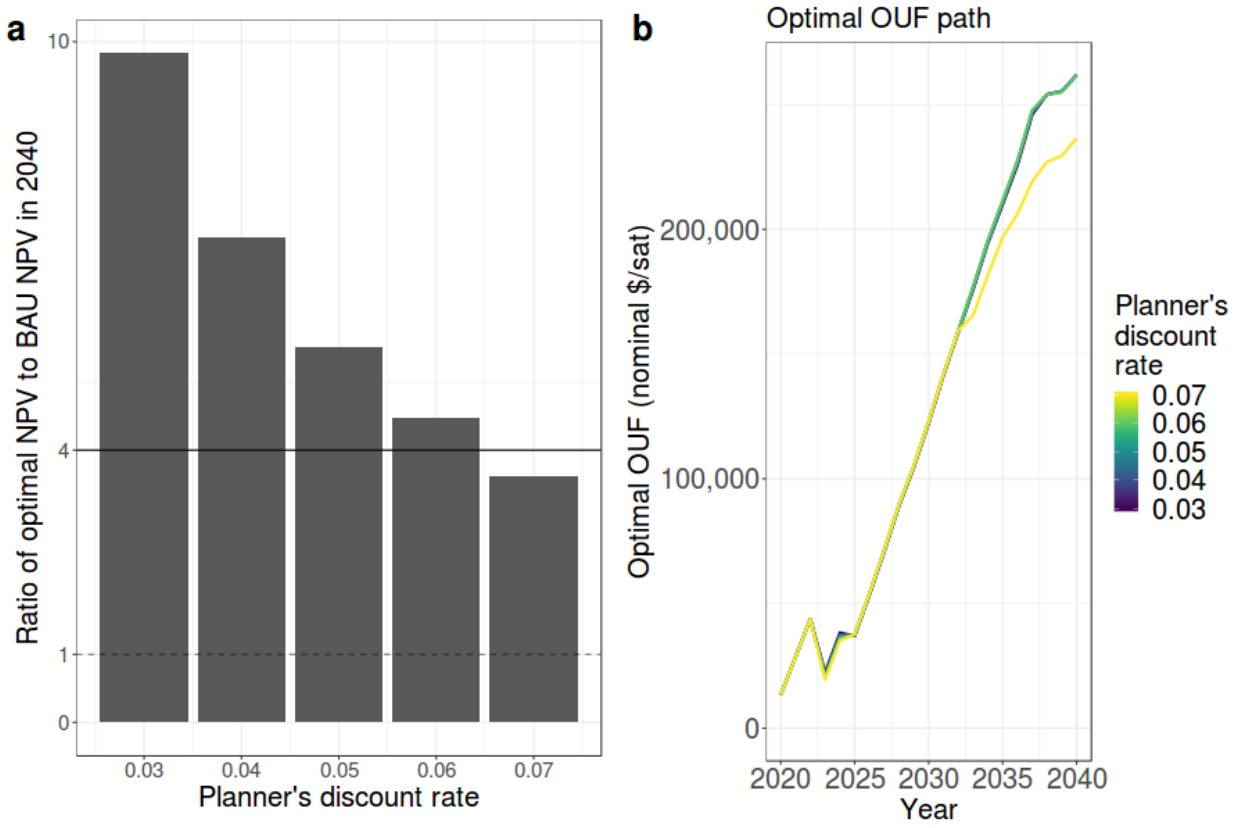


Figure S8: Discount rate sensitivity analysis. Panel a shows the ratio of optimal management NPV to BAU NPV, and panel b shows the corresponding optimal OUF paths.

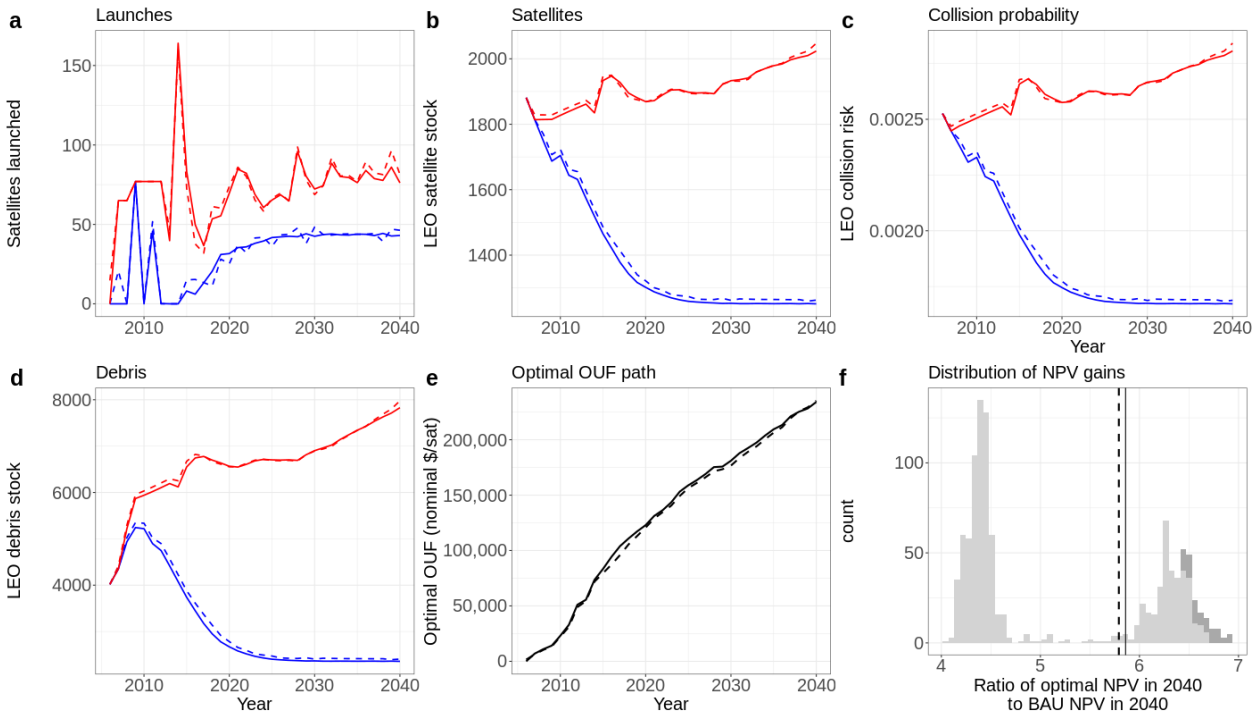


Figure S9: Grid resolution sensitivity analysis. The dashed lines show model projections with the coarse grid (64 points, 8 in satellites and debris each), and solid lines show model estimates with the fine grid (900 points, 30 in satellites and debris each). In panels a-d, the red lines show open-access paths, and the blue lines show optimal management paths beginning in 2020 from the respective open-access levels. In panel f, the light gray distribution is from the coarse grid (dashed line is main model estimate) and the dark gray distribution is from the fine grid (solid line is main model estimate).

# References


[1] M. Ansdell. Active space debris removal: Needs, implications, and recommendations for today's geopolitical environment. *Journal of Public & International Affairs*, 21:7–22, 2010.

[2] A. M. Bradley and L. M. Wein. Space debris: Assessing risk and responsibility. *Advances in Space Research*, 43:1372–1390, February 2009.

[3] Brian Weeden. History of asat tests in space, 2019. From Brian Weeden (Secure World Foundation) at `https://docs.google.com/spreadsheets/d/1e5GtZEzdo6xk41i2_ei3c8jRZDjvP4Xwz3BVsUHwi48/edit#gid=0`. Accessed January 16th 2020.

[4] Y. Cai and K. L. Judd. Stable and efficient computational methods for dynamic programming. *Journal of the European Economic Association*, 8(2-3):626–634, 2010.

[5] J. Carroll. Bounties on orbital debris? First Int'l Conf. on Orbital Debris, 2019.

[6] Combined Space Operations Center. Space-track.org satellite catalog, 2018. From Space-Track.org at `https://www.space-track.org/`.

[7] J. Duchon. Splines minimizing rotation-invariant semi-norms in sobolev spaces. In *Constructive theory of functions of several variables*, pages 85–100. Springer, 1977.

[8] European Space Agency. Discos database, 2018. From ESA at `https://discosweb.esoc.esa.int/web/guest/home`.

[9] H. S. Gordon. The economic theory of a common-property resource: The fishery. *Journal of Political Economy*, 62, 1954.

[10] A. E. Hoerl, R. W. Kennard, and R. W. Hoerl. Practical use of ridge regression: A challenge met. *Journal of the Royal Statistical Society: Series C (Applied Statistics)*, 34(2):114–120, 1985.

[11] IADC. Iadc space debris mitigation guidelines. Technical Report IADC-02-01, September 2007.

[12] A. Jonas, A. Sinkevicius, S. Flannery, B. Swinburne, P. Wellington, T. Tsui, R. Lalwani, J. E. Faucette, B. Nowak, R. Shanker, K. Pan, and E. Zlotnicka. Space: Investment implications of the final frontier. Technical report, Morgan Stanley, November 2017.

[13] D. L. Kelly and C. D. Kolstad. Integrated assessment models for climate change control. *International yearbook of environmental and resource economics*, 2000:171–197, 1999.

[14] P. Ketz. Subvector inference when the true parameter vector may be near or at the boundary. *Journal of Econometrics*, 207:285–306, December 2018.

[15] R. Klima, D. Bloembergen, R. Savani, K. Tuyls, D. Hennes, and D. Izzo. Space debris removal: A game theoretic analysis. *Games*, 7(3):20, 2016.

[16] J.-P. Kreiss and S. N. Lahiri. Bootstrap methods for time series. In *Handbook of statistics*, volume 30, pages 3–26. Elsevier, 2012.

[17] F. Letizia, C. Colombo, H. Lewis, and H. Krag. Extending the ecob space debris index with fragmentation risk estimation. 2017.

[18] F. Letizia, S. Lemmens, and H. Krag. Application of a debris index for global evaluation of mitigation strategies. 69th International Astronautical Congress, October 2018.

[19] C. Muller, O. Rozanova, and M. Urdanoz. Economic valuation of debris removal. In *68th International Astronautical Congress*, 2017.

[20] W. Nordhaus. Chapter 16 - integrated economic and climate modeling. In P. B. Dixon and D. W. Jorgenson, editors, *Handbook of Computable General Equilibrium Modeling SET, Vols. 1A and 1B*, volume 1 of *Handbook of Computable General Equilibrium Modeling*, pages 1069 – 1131. Elsevier, 2013. doi: https://doi.org/10.1016/B978-0-444-59568-3.00016-X. URL http://www.sciencedirect.com/science/article/pii/B978044459568300016X.

[21] A. Rao. *The Economics of Orbit Use: Theory, Policy, and Measurement*. PhD thesis, University of Colorado at Boulder, 2019.

[22] Union of Concerned Scientists. Ucs satellite database, 2018. From UCS at https://www.ucsusa.org/nuclear-weapons/space-weapons/satellite-database. Accessed April 2019.

[23] B. C. Weeden. Overview of the legal and policy challenges of orbital debris removal. Technical Report IAC-10.A6.2.10, September 2010.

[24] M. Wienzierl. Space, the final economic frontier. *Journal of Economic Perspectives*, 32:173–192, Spring 2018.

[25] J. Wilkerson, B. Leibowicz, D. Diaz, and J. Weyant. Comparison of integrated assessment models: Carbon price impacts on u.s. energy. *Energy Policy*, 76:18–31, 01 2015. doi: 10.1016/j.enpol.2014.10.011.

[26] H. Zou and T. Hastie. Regularization and variable selection via the elastic net. *Journal of the royal statistical society: series B (statistical methodology)*, 67(2):301–320, 2005.